AGU PUBLICATIONS

Tectonics

RESEARCH ARTICLE
10.1002/2015TC003933

Key Points:
- The Shyok suture zone formed in the early Late Cretaceous
- Final collision between India and Eurasia was not along the Shyok suture zone
- The total offset across the Karakoram fault is 130–190 km

Supporting Information:
- Texts S1–S4 and Tables S1–S3

Correspondence to:
N. L. Borneman,
nlb@asu.edu

Citation:
Borneman, N. L., K. V. Hodges, M. C. van Soest, W. Bohon, J.-A. Wartho, S. S. Cronk, and T. Ahmad (2015), Age and structure of the Shyok suture in the Ladakh region of northwestern India: Implications for slip on the Karakoram fault system, *Tectonics*, *34*, 2011–2033, doi:10.1002/2015TC003933.

Received 30 MAY 2015
Accepted 12 AUG 2015
Accepted article online 15 AUG 2015
Published online 3 OCT 2015

©2015. American Geophysical Union. All Rights Reserved.

Age and structure of the Shyok suture in the Ladakh region of northwestern India: Implications for slip on the Karakoram fault system

Nathaniel L. Borneman[1], Kip V. Hodges[1], Matthijs C. van Soest[1], Wendy Bohon[1], Jo-Anne Wartho[2], Stephanie S. Cronk[3], and Talat Ahmad[4]

[1]School of Earth and Space Exploration, Arizona State University, Tempe, Arizona, USA, [2]GEOMAR Helmholtz Centre for Ocean Research Kiel, Kiel, Germany, [3]Department of Civil and Environmental Engineering, Pennsylvania State University, University Park, Pennsylvania, USA, [4]Vice Chancellor's Office, Jamia Millia Islamia, New Delhi, India

Abstract A precise age for the collision of the Kohistan-Ladakh block with Eurasia along the Shyok suture zone (SSZ) is one key to understanding the accretionary history of Tibet and the tectonics of Eurasia during the India-Eurasia collision. Knowing the age of the SSZ also allows the suture to be used as a piercing line for calculating total offset along the Karakoram Fault, which effectively represents the SE border of the Tibetan Plateau and has played a major role in plateau evolution. We present a combined structural, geochemical, and geochronologic study of the SSZ as it is exposed in the Nubra region of India to test two competing hypotheses: that the SSZ is of Late Cretaceous or, alternatively, of Eocene age. Coarse-continental strata of the Saltoro Molasse, mapped in this area, contain detrital zircon populations suggestive of derivation from Eurasia despite the fact that the molasse itself is deposited unconformably onto Kohistan-Ladakh rocks, indicating that the molasse is postcollisional. The youngest population of detrital zircons in these rocks (approximately 92 Ma) and a U/Pb zircon date for a dike that cuts basal molasse outcrops (approximately 85 Ma) imply that deposition of the succession began in the Late Cretaceous. This establishes a minimum age for the SSZ and rules out the possibility of an Eocene collision between Kohistan-Ladakh and Eurasia. Our results support correlation of the SSZ with the Bangong suture zone in Tibet, which implies a total offset across the Karakoram Fault of approximately 130–190 km.

1. Introduction

Major late Cenozoic transcurrent fault systems offset preexisting suture zones of varied ages, which form the boundaries between tectonic elements of the Tibetan Plateau [*Yin*, 2010]. These suture zones can provide important constraints on the nature and magnitude of transcurrent tectonics on the plateau provided that they can be correlated with confidence. Unfortunately, suture zone correlations are not always straightforward, as many sutures contain similar rock associations and geochemical characteristics regardless of their ages. The most robust approach to correlating suture zones involves a comparison of the ages of oceanic rock assemblages (which provide a maximum age for a given suture zone), the ages of subduction zone metamorphic assemblages (which similarly provide a maximum age for a given suture zone), and the ages of overlapping sedimentary packages (which provide a minimum age for a given suture zone). If these three classes of ages for two apparently offset suture zones are found to be compatible, we can reasonably interpret the sutures to be offset equivalents and use that offset to constrain transcurrent slip magnitudes and long-term average slip rates. Here we apply this approach to one of the most important late Cenozoic transcurrent structures on the Tibetan Plateau—the Karakoram fault system (Figure 1).

The Karakoram fault system is a dextral transpressive structural system which strikes NW-SE and effectively marks the southwestern boundary of the Tibetan Plateau. It links four suture zones of Cretaceous-early Cenozoic age. To the east of the Karakoram fault system are the roughly E-W striking Bangong suture zone —regarded as having formed between approximately 101 and 83 Ma [*Liu et al*., 2014], and the Yarlung suture zone. Most Himalayan researchers are persuaded by the preponderance of available evidence that the Indus and Yarlung suture zones are Eocene structures [e.g., *Najman et al*., 2010; *St-Onge et al*., 2010; *Rowley*, 1996; *van Hinsbergen et al*., 2012], but some researchers have concluded that the Yarlung suture formed later (e.g., Oligocene [*Aitchison et al*., 2011]) or earlier (e.g., Late Cretaceous [*Yin and Harrison*, 2000]). To the west of the Karakoram fault system are two comparable suture zones: the NW-SE Shyok suture zone (SSZ), which can be

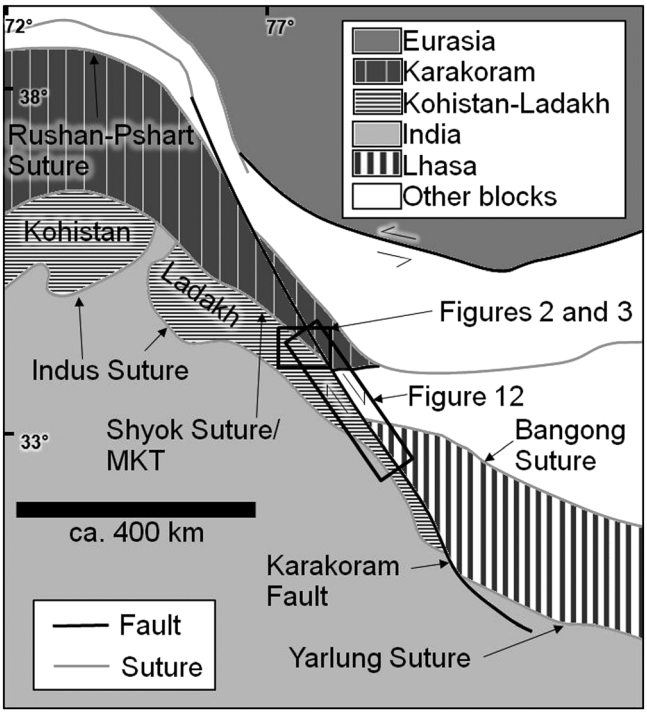

Figure 1. Regional tectonic sketch map, redrawn after *Yin and Harrison* [2000]. MKT is the Main Karakoram Thrust.

traced westward into Pakistan and north of the Nanga Parbat syntaxis as the "northern suture," and the more southern E-W Indus suture zone (ISZ) or "southern suture." Exactly how these structures might correlate across the Karakoram fault system is a fundamental problem in Himalayan-Tibetan tectonics because it has important implications for the measurement of the total offset of the central sector of the Karakoram fault system: approximately 120 km versus 200 km [e.g., *Phillips et al.*, 2004; *Valli et al.*, 2008]. A central issue in this debate is the age of the SSZ, which has been alternatively interpreted as a Cretaceous structure [*Rehman et al.*, 2011; *Robertson and Collins*, 2002; *Weinberg et al.*, 2000]—implying correlation with the Bangong suture zone—or an Eocene structure [*Bouilhol et al.*, 2013], instead implying correlation with the Yarlung suture zone. In this study, we present new structural, geochronological, and geochemical data from the Shyok suture zone as exposed in the Saltoro Range of Ladakh region of northern India (Figure 2a). Our results not only have implications for the total offset of the Karakoram fault system but also for the significance of the Shyok suture in the Mesozoic to Cenozoic India-Eurasia collision process.

2. Regional Setting

The region of interest for our study (indicated by a rectangle in Figure 1 and shown in detail in Figures 2 and 3) includes three major lithotectonic elements: the Kohistan-Ladakh block, the Karakoram block, and the intervening SSZ.

2.1. The Kohistan-Ladakh Block

The Ladakh block (Figures 1 and 3) makes up the bulk of the Ladakh Range (Figure 2a) and is comprised predominantly of calc-alkaline batholithic rocks and their extrusive equivalents (typically referred to as the Khardung Volcanic sequence), with rare pendants of preintrusive country rock [*Weinberg and Dunlap*, 2000; *Thanh et al.*, 2010]. Intrusive compositions range from gabbro to granite, while the Khardung (Kardung) Volcanics are dominantly felsic [*Dunlap and Wysoczanski*, 2002]. Two possible eastward extensions of the Ladakh block have been proposed. The most commonly made correlation is to the Mesozoic-Cenozoic Gangdese arc to the east in southern Tibet [*Ji et al.*, 2009]. The Gangdese arc is widely regarded as a continental arc developed on the southern margin of Eurasia prior to final closure of the Tethys Ocean basin [*Hodges*, 2000]. Along with its previously deformed Mesoproterozoic(?)-Mesozoic country rocks, the Gangdese arc was built on the Lhasa tectonic block of southern Tibet [*Yin and Harrison*, 2000]. Thus, the Lhasa block country rock would correlate tectonostratigraphically with Ladakh country rock in this scenario, although exposures of the host rocks for the Ladakh batholith are rare and mostly restricted to small screens making this interpretation difficult to test. A second possibility is that the eastern equivalent of the Ladakh arc is not the Gangdese arc but instead an oceanic arc that has been eroded away, overthrust, buried, or some combination of the three. In this scenario [*Bouilhol et al.*, 2013; *Aitchison et al.*, 2011], the only record of the oceanic arc in southern Tibet would be the Zedong block described by *McDermid et al.* [2002], a Jurassic igneous and volcaniclastic package distributed along the Yarlung suture zone. However, *Zhang et al.* [2014] have correlated

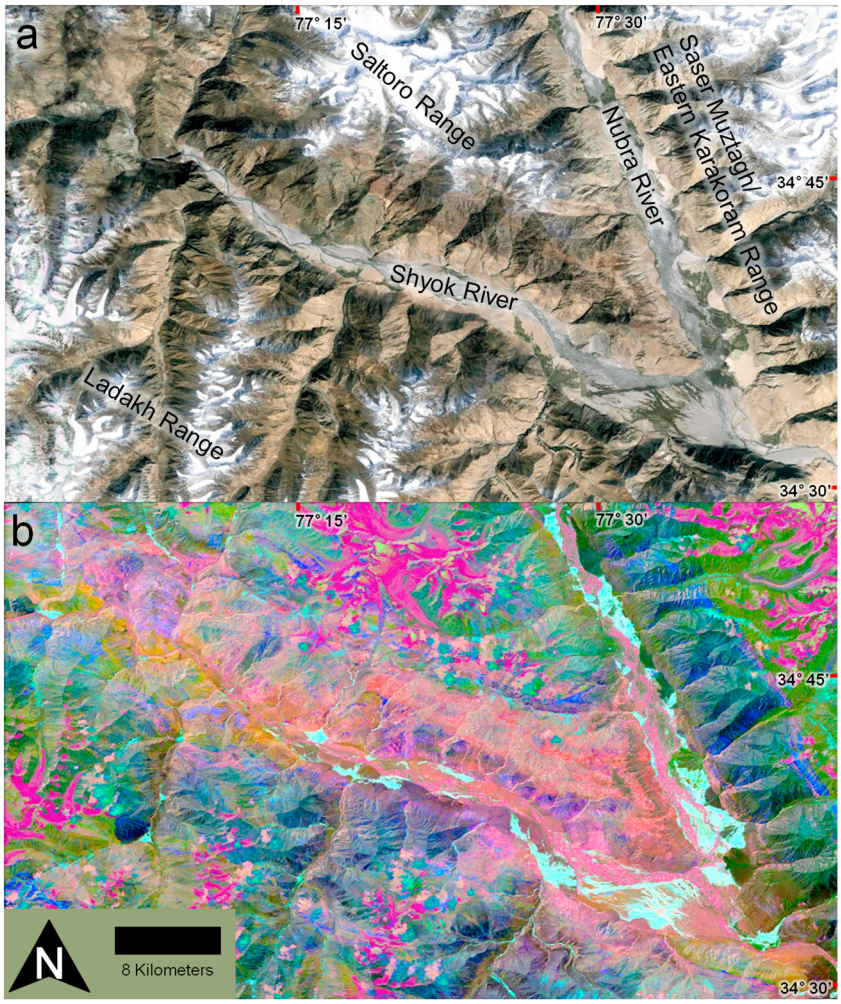

Figure 2. (a) Google Earth (map data: Google, CNES/Astrium, DigitalGlobe) image of the study area with major geographic features labeled. (b) Decorrelation stretched Landsat image of the study area which has the same field of view as Figure 2a.

the Zedong block to the Lhasa block, calling into question the need to invoke the existence of an oceanic arc in south-central Tibet.

Most researchers also regard the Ladakh batholith to be, at least in part, the eastward continuation of the Kohistan arc in Pakistan to the west [*Hodges*, 2000]. Since the Kohistan arc appears to have been intraoceanic prior to collision, the possible correlation with Ladakh implies that the later may have been transitional in nature, beginning as an intraoceanic arc that collided with either India or Eurasia and became continental thereafter [*Clift et al*., 2002; *Raz and Honegger*, 1989]. Calc-alkaline plutons of the Kohistan batholith are separated from the Ladakh intrusions by convergence of the ISZ and the SSZ around the Nanga Parbat syntaxis. The Kohistan portion of the arc formed as early as the Early Cretaceous [*Robertson and Collins*, 2002], while the majority of the Ladakh batholith intruded in Paleocene-Eocene time [*St-Onge et al*., 2010; *Weinberg and Dunlap*, 2000; *White et al*., 2011], with some components even as young as Miocene [*Bouilhol et al*., 2013]. Existing geochronologic data suggest that the Khardung Volcanics were erupted between 67.4 ± 1.1 and 60.5 ± 1.3 Ma (2σ) [*Dunlap and Wysoczanski*, 2002].

2.2. The Karakoram Block

The Karakoram block (Figures 1 and 3) includes granitoid rocks of the Jurassic to Cenozoic Karakoram batholith that intruded and metamorphosed host rocks that are referred to collectively as the Karakoram metamorphic complex [*Searle and Tirrul*, 1991; *Crawford and Searle*, 1992; *Fraser et al*., 2001; *Heuberger et al*., 2007; *Searle et al*., 2010; *Horton and Leech*, 2013]. Protoliths of metamorphic rocks in the Karakoram

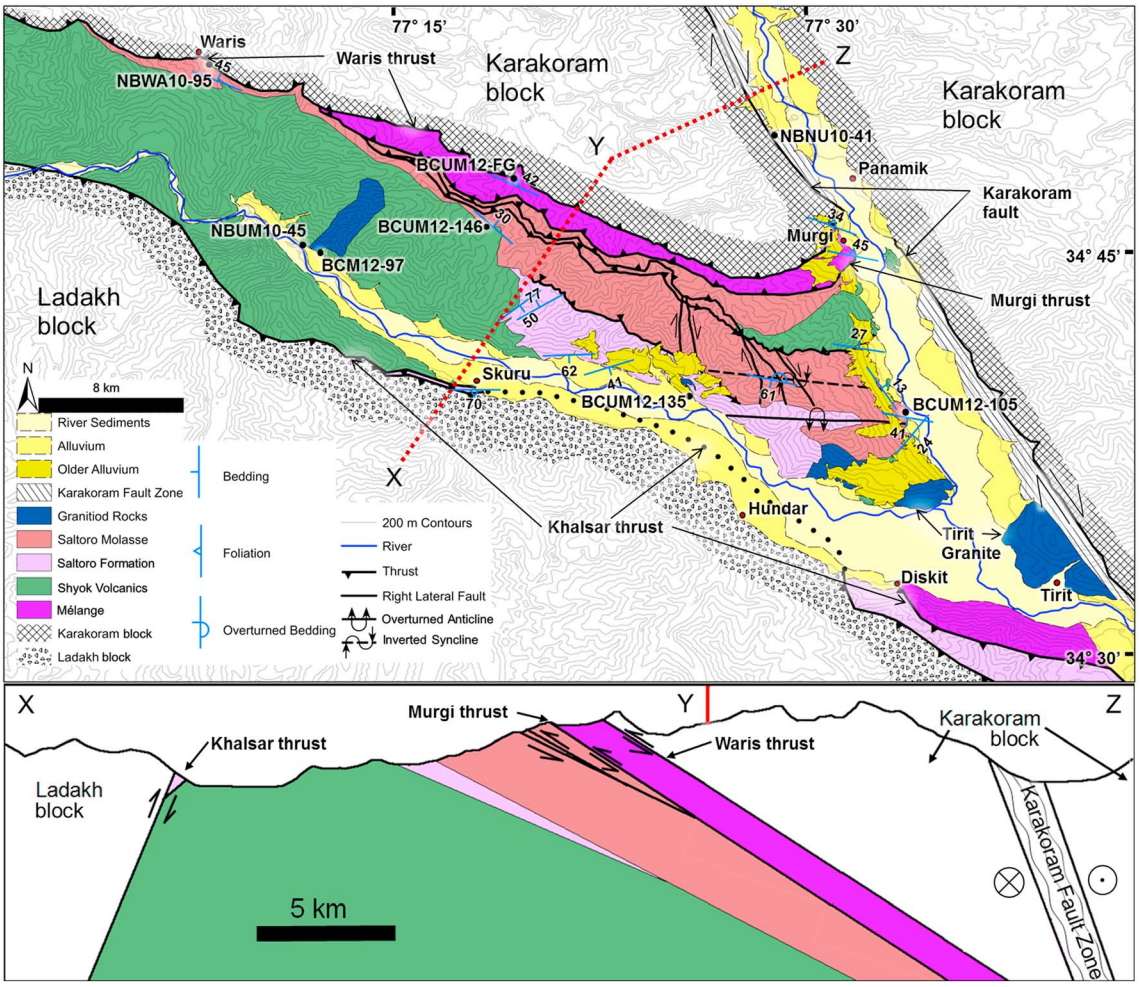

Figure 3. Geologic map and cross section of the Shyok suture zone, with the same field of view as Figures 2a and 2b. Unit colors are the same in the map and cross section, and there is no vertical exaggeration.

encompass most major rock types and sedimentary protoliths within the Karakoram block range in age from Carboniferous to Upper Cretaceous. Four main metamorphic events have been identified in the Karakoram block: a high-temperature (*T*), low-pressure (*P*) event from 63 to 50 Ma that peaked at approximately 50 Ma; a kyanite-sillimanite grade event from 40 to 22 Ma that peaked at approximately 28 Ma; a high-*T* low-*P* event from 25 to 13 Ma that peaked at approximately 21 Ma; and migmatite generation to retrograde metamorphism associated with thrusting in the Neogene [e.g., *Searle et al*., 2010]. The youngest metamorphic event formed in conjunction with slip on the Main Karakoram Thrust (MKT), a Cenozoic structure that thrusts the Karakoram block units southward over the SSZ [*Allen and Chamberlain*, 1991; *Fraser et al*., 2001]. All metamorphic events are associated with igneous rock emplacement and broadly correlate with the major magmatic episodes.

2.3. The Shyok Suture and Plausible Correlatives

The SSZ has been mapped in a narrow region of NW India and contiguous NE Pakistan between the Karakoram and Ladakh blocks. Previous work documented that the dominant rock types in the zone are basaltic ophiolitic fragments of the ocean basin that separated the Kohistan-Ladakh arc from Eurasia, as well as associated oceanic sediments of pelagic to continental shelf affinity [*Robertson and Collins*, 2002; *Rolland et al*., 2000; *Upadhyay*, 2014]. Published geochronology of rocks from the ophiolitic fragments range from approximately 134 to 104 Ma [*Khan et al*., 2009; *Thanh et al*., 2012] and place a maximum age constraint on the SSZ development. Additional constraints are provided by crosscutting igneous rocks from exposures of the SSZ in Pakistan. *Treloar et al*. [1989] inferred that SSZ formation in Kohistan is younger than the approximately

102 ± 12 Ma (2σ) Rb-Sr age of the presuturing Matum Das pluton. They considered the SSZ to be older than the approximately 75 Ma $^{40}Ar/^{39}Ar$ hornblende age of the Jutal dikes, which crosscut the SSZ and the aforementioned pluton. They further suggested that the SSZ is younger than the approximately 85 Ma metamorphism of the Kohistan-Ladakh arc. *Searle et al*. [1999] argued that the SSZ in Kohistan must be younger than the 95 Ma U-Pb zircon age of the presuturing Hunza pluton unit but older than the approximately 75 Ma Jutal dikes. A Cretaceous age for the SSZ was also inferred by *Weinberg et al*. [2000] and *Rehman et al*. [2011].

More recently, the interpretation of a Cretaceous age of the SSZ has been challenged. *Khan et al*. [2009] proposed an approximately 50 Ma age, although *Rehman et al*. [2011] dismissed their arguments on the basis that an Eocene age would require a geologically unreasonable convergence rate. Subsequently, *Bouilhol et al*. [2013] built on Khan et al.'s methodology, using Hf isotopes in zircon to detect continental input into magmas. They inferred an even younger collision between Kohistan-Ladakh and Eurasia at 40 Ma. This interpretation also figures prominently in a recent model of India-Eurasia geodynamics that features double subduction within the Tethys Ocean basin over the Cretaceous-early Tertiary interval [*Jagoutz et al*., 2015]. There is also a lack of complete consensus on the timing of final suturing between Eurasia and India. The various interpretations focus on permissible correlations among the Indus suture zone separating the Kohistan-Ladakh block from India, the Bangong suture zone separating the Lhasa block from the Qiangtang block to the north, the Yarlung suture zone separating the Lhasa block from India, and the Shyok suture zone separating the Kohistan-Ladakh block from the Karakoram block [*Schwab et al*., 2004; *Yin and Harrison*, 2000]. Of special importance in evaluating these interpretations are the ages of these sutures. Consensus has been reached only on the approximately 50–55 Ma age of the Indus suture [e.g., *Tripathy-Lang et al*., 2013; *Bouilhol et al*., 2013]. Work thus far on the Bangong suture suggests some diachroneity of activity along its strike, but—in general—it appears to be Cretaceous in age, with final closure in the 101–83 Ma range toward its western terminus against the Karakoram Fault [*Kapp et al*., 2007; *Liu et al*., 2014]. Considerable disagreement exists in the literature regarding the ages of the others.

Conventional wisdom (as reviewed by *Hodges* [2000]) holds that collision along the Yarlung suture zone occurred at approximately the same time as that along the Indus suture zone at approximately 55–50 Ma [*Najman et al*., 2010; *Rowley*, 1996; *van Hinsbergen et al*., 2012]. However, some recent papers have called that age into question. For example, *Aitchison et al*. [2011] argued for an age of collision possibly as young as approximately 35 Ma, while *DeCelles et al*. [2014] and *Wu et al*. [2014] argued for a 58–60 Ma age based on what they interpreted as a change from Indian to Asian detritus in sedimentary basins within the Yarlung suture.

2.4. Proposed Total Displacements for the Central Karakoram Fault System

As is apparent form the above background, the correct correlation of the SSZ with other sutures in Tibet would provide an important constraint on the total displacement along the central sector of the Karakoram fault system. Correlating the SSZ to the Bangong suture zone proper leads to a total offset of 120 km, consistent with proposed offsets of Karakoram block granites and the antecedent Indus River, respectively, to the north and south along strike of the Karakoram Fault [*Phillips et al*., 2004]. Correlating the SSZ with a thrust sheet of the Bangong suture zone referred to as the Shequanhe suture zone [*Kapp et al*., 2003] leads to a total offset estimate of 200 km [*Valli et al*., 2008]. *Bouilhol et al*.'s [2013] correlation of the SSZ with the Yarlung suture zone implies an offset of approximately 450 km, more or less consistent with the 480 km total offset implied by correlating the Bangong suture zone with the Rushan-Pshart suture zone to the north of the Karakoram block (Figure 1) [*Valli et al*., 2008].

Our research was motivated by a belief that better constraints on the timing of the formation of the SSZ would improve our level of confidence in how best to correlate the SSZ to the Bangong suture zone or the Yarlung suture zone and thus improve our understanding of the broader accretionary history of southern Tibet.

3. Geology of the Saltoro Range and Results

Much of the trace of the SSZ lies in a politically sensitive international border region, but the best and most accessible exposures are found in the Saltoro Range of NW India. The geologic basis for our work was developed by field mapping and sample collection over 3 months in 2010 and 2012 (Figures 2 and 3). The study area is, for the most part, extremely rugged, and some important outcrops are difficult to access.

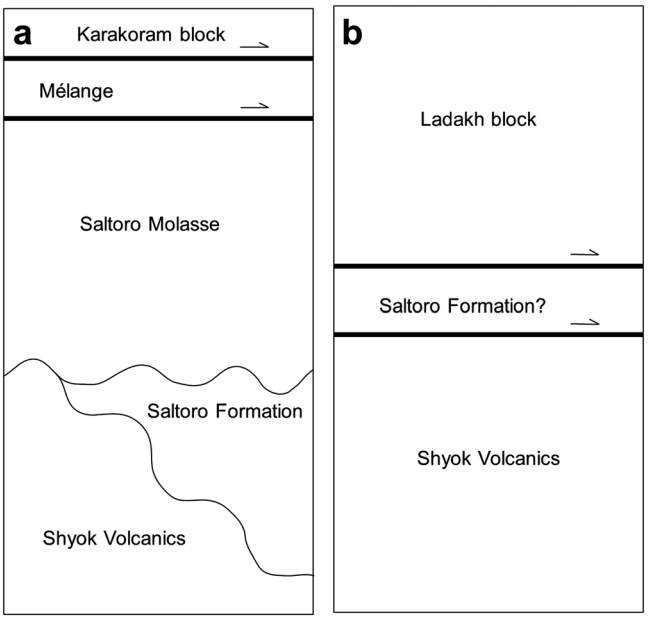

Figure 4. Schematic tectonic stratigraphy showing the relative positions of major units seen in the mapping area (a) within the Saltoro Range and (b) near the town of Skuru on the northern margin of the Ladakh batholith.

As a consequence, we augmented field observations with remote sensing data analysis. NASA's *Reverb ECHO* service was used to select a Landsat 7 scene (LE71470362000241SGS00) with minimal snow and cloud cover in the region of interest. All processing was done using the *ENVI* software suite. The scene was clipped to the vicinity of the Saltoro Range in order to focus any processing on the region of interest. Our image processing methods follow those of *Cooper et al*. [2012] adapted for Landsat imagery which has similar visible and infrared spectral coverage to the Advanced Spaceborne Thermal Emission and Reflection Radiometer imagery used in that study. Heavily vegetated regions were masked out. All spectral bands were then processed using principal component analysis [*Cooper et al*., 2012; *Jolliffe*, 2002], and three bands showing the least influence of topography and shadow and the best opportunity for distinguishing different lithologies were combined into a single image. This image was then combined with the higher-resolution band 8 from the original unstretched image to produce a higher-resolution final image. Google Earth imagery (Figure 2a) and the final decorrelation-stretched Landsat image (DSI; Figure 2b) were used as base maps for field mapping, which permitted us to correlate colors on the DSI with observed lithologies. These correlations then permitted us to extend the mapping to regions of the Saltoro Range that were otherwise inaccessible. Throughout the area, heavy dust cover and desert varnish mask the characteristic spectral data of various rock types to varying degrees, making it difficult to robustly interpret the spectral data. However, sharp color changes in the remote sensing image were found to be highly indicative of lithologic change. Based on a combination of field observation and remote sensing data interpretation, we classified five mapping units within the SSZ; their distributions and relationships are shown on the geologic map and illustrative cross section in Figure 3 and simplified tectonostratigraphic columns in Figure 4.

3.1. Ladakh Block Lithologies

The Ladakh block forms the southernmost portion of the study area, where it is thrust over the SSZ along a south dipping fault (Figure 3). The Ladakh block primarily consists of coarse- to fine-grained granites to diorites with K-Ar biotite ages of approximately 66–49 Ma with abundant associated hornfels of coincident age [*Thanh et al*., 2010]. Included in this tectonostratigraphic block is the approximately 67.4–60.5 Ma Khardung Volcanic unit, which overlies and is interpreted to be the volcanic equivalent of the Ladakh affinity granitoids within the block [*Dunlap and Wysoczanski*, 2002].

3.2. Shyok Suture Zone Volcanic and Sedimentary Units

Historically, names for extrusive igneous and low-grade metaigneous rocks, as well as associated sedimentary and low-grade metasedimentary rocks in the SSZ, have been inconsistently applied [e.g., *Rai*, 1982; *Rolland et al*., 2000; *Weinberg et al*., 2000; *Juyal*, 2006; *Ehiro et al*., 2007; *Thanh et al*., 2012; *Upadhyay*, 2014]. For example, a volcanic or volcaniclastic unit that may or may not include serpentinite-bearing mélanges may variably be mapped as the Shyok Volcanics, Shyok Formation, Nubra Formation, Saltoro Andesite, Tsoltalk-Shyok Formation, and Mélange Unit. With the exception of a relatively consistently recognized molassic conglomerate, sedimentary rocks in Nubra are variably referred to as Flysch, Tsoltak Formation, Saltoro Flysch Formation, Hundiri Formation, Sedimentary Unit, Tsoltalk-Shyok Formation, and Saltoro Formation.

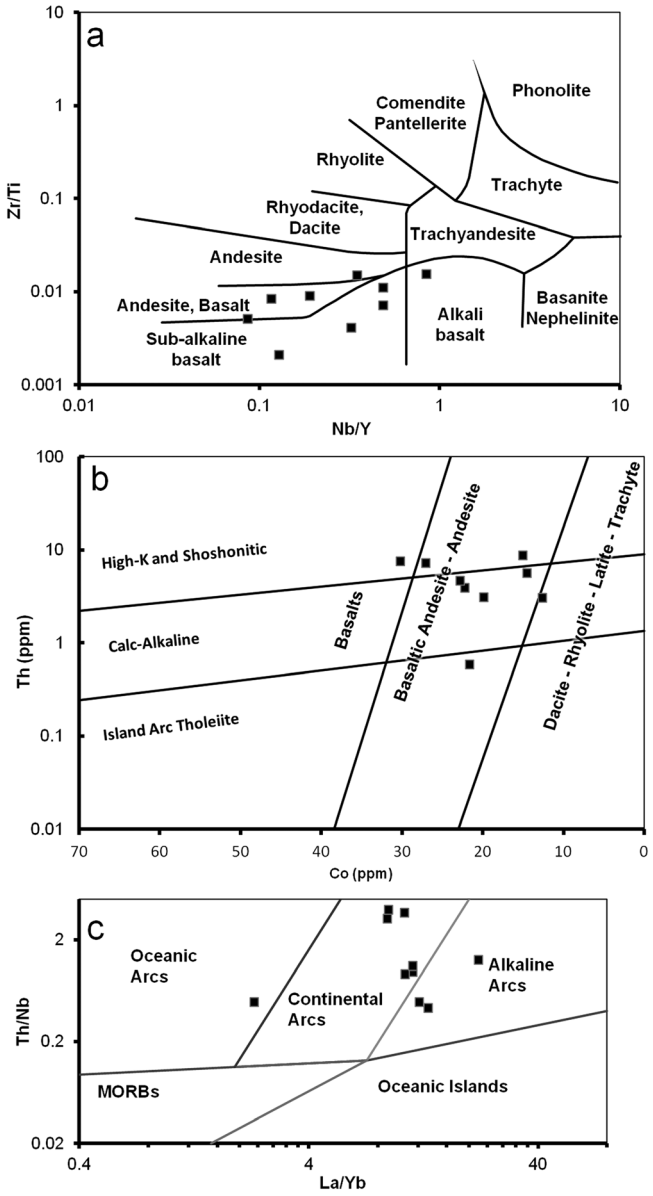

Figure 5. Classification diagrams for the Shyok Volcanic unit after (a) *Winchester and Floyd* [1977], (b) *Hastie et al*. [2007], and (c) *Hollocher et al*. [2012]. The black squares are data from Shyok Volcanic rocks analyzed for our study.

Much of the confusion of units in the region likely results from limited access within the Saltoro Range itself, forcing prior workers to attempt correlation of rocks from the bank of the Nubra River to rocks from the south bank of the Shyok River (Figure 2a) without knowledge of the intervening geology. For the purpose of this discussion, we choose to divide units based on geologic/tectonic environment. At the same time, we do not wish to introduce further nomenclature to an already confusing situation. Therefore, for the most part, we choose to denote units based on the nomenclature of *Upadhyay* [2014].

3.2.1. Shyok Volcanics of the Saltoro Range

The structurally lowest exposed units in the study area are lower greenschist facies metavolcanic and metavolcaniclastic rocks (shown in green in Figure 3). These are typically green in outcrop, but altered exposures can be bright to dull earthy orange. The bottom of the Shyok Volcanic unit is not observed, placing its minimum thickness at 2 km. Protolith lithologies include intermediate to mafic volcanic rocks and less common interlayered volcanogenic sedimentary rocks [*Weinberg et al*., 2000]. Most exposures contain massive porphyritic rocks of intermediate composition that locally display relict-brecciated texture indicative of emplacement as block and ash flows. Common metamorphic assemblages are plagioclase + epidote + chlorite + actinolite + quartz + calcite + opaques ± sphene with relict pyroxenes, biotite, and hornblende. Alteration is common, with veins consisting of quartz, calcite, and oxides with occasional sulfides and Cu mineralization. Toward the northwestern portion of the study area along the Shyok River, the Shyok Volcanic unit is intruded by gabbroic rock and hornblendite dikes oriented perpendicular to bedding. These dikes are interpreted to be hypabyssal equivalents to the Shyok Volcanics.

Evidence of both metamorphism and localized alteration suggest that robust classification and tectonic setting discrimination of these rocks must be based on relatively immobile trace elements. We performed such analyses on representative samples (see supporting information section for details and Table S1 in the supporting information for data). Figure 5 illustrates salient features of the results using Zr/Ti versus Nb/Y, Th versus Co, and Th/Nb versus La/Yb diagrams [*Winchester and Floyd*, 1977; *Hastie et al*., 2007; *Hollocher et al*., 2012]. For the most part, the analyzed samples are best described as subalkaline basalts or andesites following a primarily calc-alkaline trend (Figures 5a and 5b). All but one sample fall within the continental arc or alkaline arc fields of the Th/Nb versus La/Yb discrimination diagram proposed by *Hollocher et al*. [2012] (Figure 5c), consistent with a pre-India-Eurasia collision, arc-magmatic origin for the Shyok Volcanics.

Due to similar grade and composition, volcanic rocks north of the Khalsar thrust that underlie the Saltoro Molasse are here grouped together as the Shyok Volcanic unit. The Shyok Volcanic unit does not include any sort of mélange, such as the metavolcanics of *Thanh et al*. [2012]. The Shyok Volcanic unit includes all volcanic outcrops in the Ladakh Range west of Skuru and similar greenschist outcrops in the Saltoro Range. A major source of confusion in the region is the structural juxtaposition of the Shyok Volcanic unit, Khardung Volcanic unit, and an ophiolite-bearing mélange within a few kilometers of the confluence of the Shyok and Nubra Rivers [*Rolland et al*., 2000; *Upadhyay*, 2014; *Weinberg et al*., 2000]. We approached this problem by mapping into this area of structural complexity from areas that are less complicated but not well studied. We therefore feel that our mapping provides a better representation of the distribution of rock units.

3.2.2. Saltoro Formation

An unconformity (Figure 4a) separates the Shyok Volcanic unit from the overlying Saltoro Formation [*Upadhyay*, 2014]. The Saltoro Formation (shown in lavender in Figure 3) consists of interstratified carbonate rocks, sandstones, and mudstones. In the Saltoro Range, carbonate rocks dominate basal portions of the formation but decrease in abundance upward before becoming totally absent in the topmost exposures. In outcrop, the carbonate rocks are black to light gray, sandstones are buff, and mudstones are light gray. Bedding is on the centimeter to meter scale. Outcrops are largely transposed by subsequent deformation (see below) but, in places, possess preserved sedimentary structures showing normal graded bedding, dewatering features, and fossils. Fossils in limestone layers such as *Horiopleura haydeni*, *Eoradiolites gilgitensis*, *Cyclamina* sp., and *Numulites* sp. suggest a middle Cretaceous or older age [*Rai*, 1982; *Upadhyay*, 2014]. The maximum observed thickness of the Saltoro Formation is 3 km; however, the extent of thickening or thinning within the Saltoro Formation as a consequence of deformation is unconstrained.

We group all marine sedimentary rocks within the Saltoro Range as the Saltoro Formation due to their similar depositional environment. Some workers further group the Shyok Volcanic unit and Saltoro Formation together as the Tsoltalk-Shyok Formation [e.g., *Thanh et al*., 2012] or simply the Shyok Formation [e.g., *Weinberg et al*., 2000]. This grouping is defensible based on the likely similar age and depositional contact between the two rock types. We choose to split the rocks into two units because the sharp transition from volcanic rocks to marine sedimentary rocks, even on the remote sensing images, makes doing so straightforward. The combination of volcanic rocks and shallow marine sediments suggests an island arc environment for the eruption of the Shyok Volcanics and deposition of the Saltoro Formation [*Upadhyay*, 2008; *Upadhyay*, 2014].

3.2.3. Saltoro Molasse

The Saltoro Molasse (shown in red in Figure 3) is separated from the underlying Shyok Volcanic unit and Saltoro Formation by a buttress unconformity (Figure 4a). This contact is exposed along the Nubra River and interior of the Saltoro Range; however, along much of the southern side of the Saltoro Range along the Shyok River a presumably small offset thrust separates the Saltoro Molasse from the Saltoro Formation. The Saltoro Molasse [*Rai*, 1982], presenting as approximately 10 m thick layers of conglomerates and coarse sandstones, is typically pink to red, with local alteration to light green. The primarily clast-supported conglomerates have clast sizes ranging from 1 cm to 1 m, averaging ~10 cm. The majority of clasts are volcanic, resembling the Shyok Volcanic sequence and other local greenschist facies volcanic rocks, with subordinant granite, phyllites, and schist clasts. The sandstone beds are usually massive but occasionally show centimeter-scale bedding. The unit as a whole is oxidized, giving it a characteristic red color. Based on the preceding observations, the Saltoro Molasse is interpreted to have been deposited in a proximal alluvial fan system. This is in stark contrast to the underlying yet similarly named marine Saltoro Formation. The minimum thickness of the molasse is 3.2 km.

3.2.4. Mélange

Highest within the Shyok suture zone, an approximately 1 km thick, low-grade structural Mélange unit (shown in purple in Figure 3) with a metaphyllitic matrix has been emplaced over the Saltoro Molasse on a late, post-SSZ thrust fault described below as the Murgi thrust. Within the matrix are decimeter- to kilometer-scale blocks of phyllite, limestone, red chert, basalt, gabbro, and peridotite. Greenschist facies assemblages are common throughout the matrix but are only developed in the blocks when bulk compositions are appropriate. We have no direct constraints on the relative ages of this unit and other SSZ units, nor do we have direct constraints on its structural relationship with other SSZ units prior to development of the Murgi thrust.

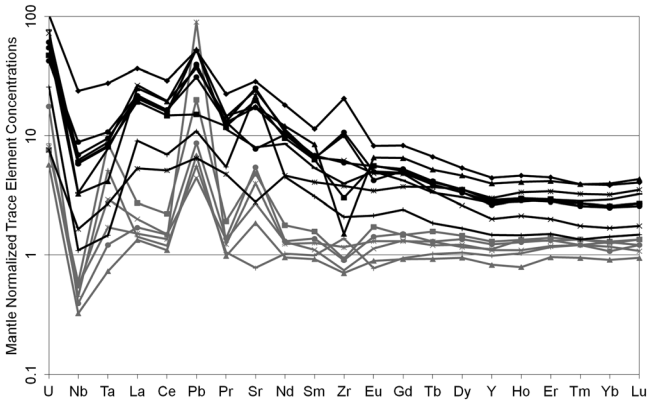

Figure 6. Trace element geochemistry for the Shyok Volcanics (black) and ophiolites from within the SSZ (gray). Data from this study and *Thanh et al.* [2012], respectively.

3.3. Late Intrusive Igneous Rocks Cutting the SSZ

All SSZ units except the Mélange unit are intruded by numerous decimeter- to meter-scale, fine-grained, felsic to mafic dikes. Some individual dikes can be traced over 1 km in the field. The felsic to intermediate composition dikes typically have an aplitic texture and are often heavily altered and crumbly in hand sample.

Several larger granitic bodies (shown in blue in Figure 3) intrude the Saltoro Formation and Shyok Volcanics. The best studied of these bodies is the Tirit Granite, found at the confluence of the Shyok and Nubra Rivers, which has an exposed outcrop area of approximately 20 km^2. Within the Saltoro Range, the Tirit "granite" is predominantly medium-grained biotite granite to granodiorite with lesser amounts of aegerine diorite. The Tirit Granite has been described geochemically as showing an arc igneous trend [*Rao and Rai*, 2009].

Two more granitic bodies within the SSZ of comparable size to the Tirit Granite were identified in this study. A hypabyssal, homogenous, fine-grained granite containing dendritic muscovite and miarolitic cavities (sample BCUM12-135) intrudes the Saltoro Formation. The age of a sample from this granite (BCUM12-135) was determined as part of this study (see section 5.3.3). In addition, a composite pluton with a wide variety of lithologies including calcite-bearing hornblende gabbros, cumulate hornblende gabbros, and diorites intrudes the Shyok Volcanics. A sample from this unit (BCUM12-97) was also dated, and the results are also reported in section 5.3.3.

3.4. Karakoram Block Lithologies

The structurally highest rock exposures in the study area are of Karakoram block units (Figure 4a), which are thrust over all of the SSZ units. Many of the highest exposures have proven difficult to access, but the rocks exposed there can be identified from observations of rockfalls from known locations when direct access was not possible. The majority of the Karakoram block in the Saltoro Range is composed of high-grade metasedimentary quartzites, schists, gneisses, migmatites, and granitoid rocks which are not differentiated on Figure 3. The typical metamorphic assemblage we observed in metapelitic and metapsammitic schists, gneisses, and migmatites is quartz + muscovite ± biotite ± plagioclase ± K-feldspar. Granitic rocks ranged from tourmaline-garnet pegmatitic leucogranites to biotite-hornblende-sphene granodiorites. Similar intrusive igneous rocks are observed near Panamik along the more accessible east bank of the Nubra River, adjacent to the Karakoram fault zone [*Ravikant et al.*, 2009; *Thanh et al.*, 2010].

3.4.1. Correlations Within the Shyok Suture Zone

The nominally calc-alkaline Shyok Volcanic unit has a distinct geochemistry from the boninite-bearing ophiolitic greenschist metavolcanic units described by *Thanh et al.* [2012] as part of the SSZ, here mapped as part of the Mélange unit. Those rocks, which are exposed to the east of the study area, have geochemical characteristics more consistent with eruption in a fore-arc basin environment instead of the likely arc environment of the Shyok Volcanic unit. With respect to trace elements, for example (Figure 6), the Shyok Volcanic unit is generally more enriched and lacks the distinct Pb enrichment found in the ophiolitic metavolcanics. While *Thanh et al.* [2012] regarded some rocks within our map area as having an ophiolitic character, we mapped them instead as part of the Shyok Volcanic unit. The Shyok Volcanic unit is chemically much more similar to the alkaline Khardung Formation [*Clift et al.*, 2002; *Rolland et al.*, 2000]. However, the two units have radically different ages: Cretaceous or older for the Shyok Volcanics (as constrained by the fossil age from the depositionally overlying Saltoro Formation [*Upadhyay*, 2014]) versus approximately 67.4–60.5 for the Khardung Formation [*Dunlap and Wysoczanski*, 2002].

Along the Shyok suture zone in the Baltistan region of Pakistan, the Pakora Formation's lower volcanogenic member [*Robertson and Collins*, 2002] is broadly similar to the Shyok Volcanics. For example, their described

basaltic to andesitic composition, lack of pillow lavas, and massive to volcaniclastic morphology are similar to those we have documented in the Shyok Volcanic succession; therefore, we tentatively correlate these two units.

Likewise, the Pakora Formation limestone member, along with the base of the Pakora Formation's upper volcanogenic member, is likely correlative to the Saltoro Formation. Both contain similar limestones, sandstones, and shales and have similar ages, as *Robertson and Collins* [2002] reported rudist-bearing fauna in the limestone layers of the Pakora Formation indicative of a Cretaceous (post-Valanginian) age.

Robertson and Collins [2002] also reported the existence of molasse and mélange units in the Baltistan region, providing lithologic descriptions that suggest correlation to the Saltoro Molasse and Mélange unit in our study area. However, if this correlation is correct, the relative structural position of the units is reversed: in Baltistan, the mélange sits below the molasse unit and is separated from it by north dipping reverse faults. This reversal of tectonostratigraphic positions of the two units seems plausible given the documented activity of younger thrust faults in the region, including those related to the late Cenozoic Main Karakoram thrust system [*Fraser et al*., 2001; *Robertson and Collins*, 2002].

4. Structural Geology

Major thrusts separate the study area into four blocks with differing histories: the Ladakh block, stratified and volcanic rocks of the SSZ (Shyok Volcanics, Saltoro Formation, and Saltoro Molasse), the SSZ Mélange unit, and the Karakoram block. Below we describe structures both internal to and separating these blocks.

4.1. Deformational Features of the Ladakh Block

Relatively little of the Ladakh block is exposed in our study area, but the rocks we observed were largely granitic and displayed predominately igneous textures. Locally developed planar fabrics within the block are likely magmatic in origin. Some exposures of genetically associated, low-grade metavolcanic rocks (Khardung Volcanics) were mapped just to the southeast of the study area by *Weinberg et al*. [2000], and these displayed a weak, 50°–60° north dipping cleavage.

4.2. Khalsar Thrust

The contact between the Ladakh block and stratified rocks of the SSZ is mapped as the Khalsar thrust [*Weinberg et al*., 2000] (Figures 3 and 4b). At the classic exposure of the thrust, near the town of Khalsar and southeast of the study area, the structure was mapped as striking northwest and dipping northeast, placing Shyok suture zone rocks over Khardung Volcanics of the Ladakh block. This exposure of the Khalsar thrust is of very limited extent (only a few kilometers along strike), and it becomes covered to the northwest by modern sediments along the Shyok River. Farther northwest, near Diskit, the structure is exposed and has been mapped by *Rolland et al*. [2000] as a fault zone with two principal, SW dipping strands separated by a 300–3000 m thick slice of deformed sedimentary rock. *Upadhyay* [2014] correlated these sediments to the Saltoro Formation. The fault once again strikes beneath modern sediments before reemerging in our study area. Here the fault strikes NW, dips ~70°SW, and places the Ladakh block granitic rocks over deformed phyllites that we correlate to the Saltoro Formation. It is marked by a highly deformed zone roughly 200 m thick, and hanging wall rocks in this zone, especially near the contact with the footwall, display cataclastic textures. Footwall rocks of the Saltoro Formation contain a strong phyllitic fabric subparallel to the contact. S-C planar fabrics in these rocks [*Lister and Snoke*, 1984], defined by chlorite and sericite, along with a prominent SW plunging stretching lineation, confirm that this structure is a reverse fault. The hanging wall-to-the-NE shear sense and the observation that the hanging wall here contains Ladakh block lithologies argue against the correlation of this structure with the Main Karakoram Thrust, as proposed by *Weinberg et al*. [2000]. As noted below, we regard the structurally higher Waris thrust (described in section 4.6) to be a more likely candidate for correlation with the Main Karakoram Thrust.

4.3. Deformational Features of Stratified and Volcanic Rocks of the Shyok Suture Zone

Both the Shyok Volcanic unit and the Saltoro Formation were subjected to greenschist facies metamorphism subsequent to deposition. Synmetamorphic deformational fabrics (predominately a moderately northwest dipping cleavage) can be found in most outcrops of the Saltoro Formation but are not well developed in the more massive Shyok Volcanics. Outcrop and thin section examination suggests that the Saltoro

Molasse displays no obvious deformational fabrics and does not appear to be metamorphosed. We infer that the metamorphic fabrics found in the lower units of this structural block predate molasse deposition.

The well-defined thick bedding of the Saltoro Molasse makes that unit especially useful for characterizing the internal deformation of the rocks between the Khalsar thrust and the Murgi thrust, the next higher major thrust at the base of the Mélange unit (described below). A large, overturned anticline-syncline pair was observed near the confluence of the Nubra and Shyok Rivers that affects both the molasse and the underlying Saltoro Formation. The axial planes of both folds strike roughly E-W and dip to the south. Neither structure could be traced eastward across the Shyok Valley and into the Shyok Volcanics or the structurally higher Ladakh block, and they are presumed to be internal to the suture zone sedimentary successions. The folds are cut locally by younger, steep, brittle faults that can be traced in the remote sensing imagery for several kilometers along their N-S to NW-SE strikes but appear to have minor offsets. These structures appear to be truncated by a family of thrust faults that strike WNW-ESE, locally subparallel to bedding, and dip moderately (approximately 35°) to the northeast. In most instances, these thrusts appear to duplicate parts of the Saltoro Molasse sequence, but the basal structure, near its easternmost exposure, thrusts Shyok Volcanics over Saltoro Molasse and thus has appreciable offset. This family of structures is truncated to the northwest by the thrust at the base of the SSZ Mélange unit. A similarly oriented thrust is found along one exposure of the base of the Saltoro Molasse, as noted previously by *Upadhyay* [2014]. We mapped this disrupted segment of the unconformity over a distance of roughly 20 km along strike, but its displacement appears to be minor and it dies out to the NW into the unconformity that characterizes the base of the molasse elsewhere.

4.4. Murgi Thrust

The newly named Murgi thrust places structurally chaotic rocks of the Mélange unit over the Saltoro Molasse (Figure 3). The Murgi thrust is interpreted as being responsible for carrying the SSZ Mélange unit from a structurally deeper position within the SSZ to its current structural position above the Saltoro Molasse. The Murgi thrust strikes WNW-ESE and dips 35° northward. Older deformational fabrics within the hanging wall are transposed into near parallelism near the Murgi thrust, but we were unable to definitively recognize primary thrust-related fabrics in the basal parts of the hanging wall. However, the typically weakly to unfoliated molasse lithologies of the footwall pick up a moderate to strong cleavage near the thrust. Clasts in the molasse near the contact become rotated in a way consistent with thrust sense (hanging wall to the southeast). In the northwestern part of the study area, the Murgi thrust appears to be cut by the Waris thrust or plausibly merges with it.

4.5. Deformational Features of the SSZ Mélange Unit

Although some of the larger blocks of appropriate mineralogy contain older foliations, other (more massive) blocks do not. The predominant planar fabric of the SSZ Mélange unit is a strongly developed schistosity in its matrix. This schistosity, defined by chlorite and sericite, typically strikes WNW-ESE and dips moderately (~45°) to the NE. Lineations trending ~N35°E but variably plunging are found in some outcrops. The ages of these fabrics are unclear, but the fact that they cannot be traced beyond outcrops of the SSZ Mélange unit and into surrounding units implies that they formed during mélange development or, plausibly, earlier and within the precollisional subduction complex along the southern margin of the Karakoram arc.

4.6. The Waris Thrust

The structurally highest major thrust in the Saltoro Range (Figure 3)—referred to informally here as the Waris thrust—places rocks of the Karakoram block over various units of the SSZ. This WNW-ESE striking fault dips shallowly (5–30°) northward. The thrust appears to maintain a more-or-less uniform structural position within its hanging wall but cuts downward into the footwall from east to west; in the eastern Saltoro Range, the Mélange unit forms the immediate footwall, but the Saltoro Molasse and, eventually, the Shyok Volcanics appear beneath the thrust toward the west, indicating tilting of the footwall prior to hanging wall emplacement. The structure strikes and dips similarly to the Murgi thrust and minor thrusts within the stratified and volcanic rocks of the SSZ. The intersection between the Waris and Murgi thrusts was not observed in the field, but remote sensing imagery is consistent with a merger of the two—perhaps suggesting that they are coeval—or that the Waris thrust cuts the Murgi thrust at a very low angle, which would indicate that the latter structure is at least slightly older. A roughly 10 m thick fault zone characterizes the trace of the Waris thrust. Within this zone is a localized S-C composite fabric—defined by chlorite and sericite—that strikes parallel to the fault

zone, as well as a mineral lineation that is presumed to have developed synchronously. These fabrics indicate hanging wall-to-the-southeast shear sense. They are deformed, at least locally, by a second crenulation cleavage not observed in other Saltoro Range lithologies.

Hanging wall and footwall lithologies and the eastward vergence of the Waris thrust are similar to those characterizing the classic Main Karakoram Thrust (MKT; Figure 1) mapped to the west in northern Pakistan [*Rex et al*., 1988; *Searle*, 1991; *Searle et al*., 2010], and we propose that the Waris thrust represents the eastward continuation of the MKT.

4.7. Deformational Features of the Karakoram Block

Rocks in the hanging wall of the Waris thrust (MKT) were observed only in a limited number of places. Most exposures are in the higher elevations of the Saltoro Range to which access was not possible, but we were able to sample and date rockfall from the hanging wall. Unfortunately, we know little about the outcrop orientation of these samples, and we can only describe the fabrics. Metasedimentary rocks display typical gneissosities and schistosities defined by muscovite and biotite, whereas the intrusive igneous rocks do not typically show penetrative fabrics. The igneous textures of granitic rockfall samples are similar to the "Nubra-Siachen leucogranite" described by *Phillips and Searle* [2007], which are exposed immediately east of the Karakoram fault zone in the Saser Muztagh subrange (Figure 2) of the Eastern Karakoram. Many of the fabrics within the metasedimentary rockfall samples are similar to rocks described from the Saser Muztagh for rocks described by *Van Buer et al*. [2015] as characteristic of the footwall of their Angmong Fault.

4.8. Deformational Features of the Karakoram Fault System

The NW-SE striking, dextral-oblique slip, Karakoram fault system generally occupies the valley of the Shyok River east of the Saltoro Range and separates Karakoram block units from the Karakoram Range proper. Numerous papers have been published describing the Karakoram fault system and its evolutionary history based on studies undertaken east and southeast of our study area [e.g., *Searle et al*., 1998; *Brown et al*., 2002; *Phillips et al*., 2004; *Rolland et al*., 2009], and the reader is referred to them for details. Although the earliest deformational fabrics associated with this fault are of Miocene age, it remains active today.

On the extreme eastern edge of the Saltoro Range, along the west bank of the Shyok River, we observed highly strained rocks recognizable as representative of the Karakoram block and SSZ units that contain greenschist facies tectonite fabrics with appropriate orientation to have been produced during Karakoram fault slip. We map these as a distinctive Karakoram fault zone unit. Rocks in this unit display a strong, subvertical shear fabric striking NW-SW, parallel to the Shyok Valley and inferred general strike of the Karakoram fault system. Especially in fine-grained, metasedimentary lithologies, the planar fabrics are composite and S-C relationships indicate a component of NE side up displacement in addition to dextral slip. Earlier fabrics in components of this unit derived from Karakoram block lithologies, Saltoro Formation, Saltoro Molasse, and SSZ Mélange units are transposed into parallelism with the Karakoram Fault shear fabrics, and fabrics of this orientation can be traced for meters to tens of meters across the diffuse SW boundary of the Karakoram shear zone. The youngest structures interpreted to be associated with the Karakoram Fault shear zone are numerous subvertical brittle fault zones with uncertain displacement, found within the Saltoro Range within 10 km of the Nubra River. These structures are oriented parallel to the regional orientation of the Karakoram fault system.

5. Geochronology

The $^{40}Ar/^{39}Ar$ hornblende and U/Pb zircon geochronology, as well as U/Pb geochronology of detrital zircons, provide constraints on the ages of units and major faults in the field area and the provenance of the Saltoro Molasse. Uncertainties on all new dates presented in this paper are reported at the 2σ (approximately 95%) confidence level. See the supporting information section for a description of analytical methods for the geochronologic methods used in this paper and Tables S2 and S3 for run data.

5.1. The $^{40}Ar/^{39}Ar$ Constraints on the Age of the Shyok Volcanics

Our Shyok Volcanic eruptive rock samples contained no magmatic zircon suitable for U/Pb dating. Our best available constraint on the age of the unit comes from a $^{40}Ar/^{39}Ar$ hornblende age on one of the crosscutting hypabyssal dikes (NBUM10-45). The Ar isotopes degassed from 12 incremental heating steps all yielded Early

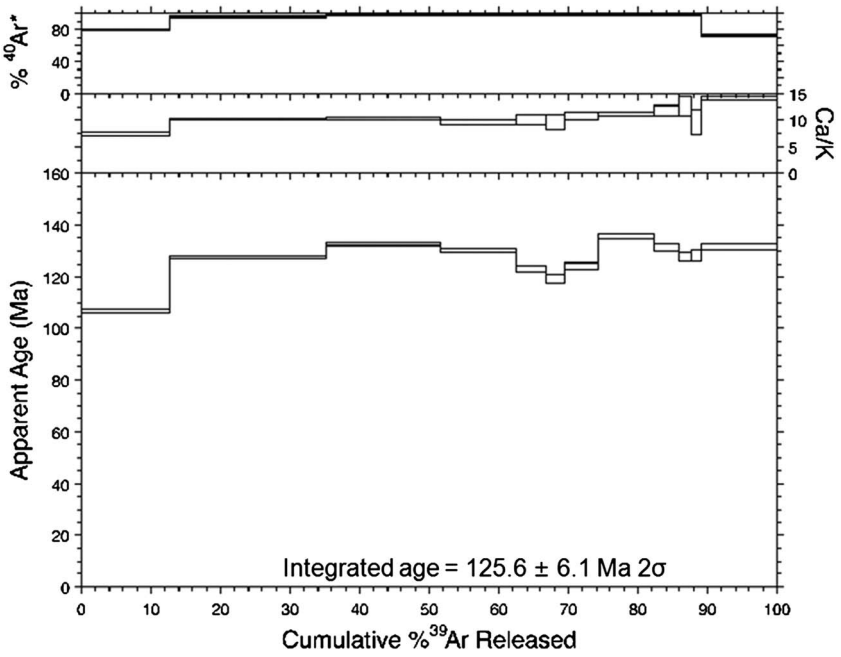

Figure 7. The $^{40}Ar/^{39}Ar$ step heating age spectrum, Ca/K ratios, and percent radiogenic ^{40}Ar ($^{40}Ar^*$) for hornblende sample NBUM10-45, sampled from a dike within the Shyok Volcanics. The box heights shown for individual steps represent 2σ errors.

Cretaceous apparent ages, but the release spectrum for this sample does not display a statistically defined plateau age (Figure 7). We refer this behavior to be indicative of contamination by a nonradiogenic, or "excess," ^{40}Ar component [*Kelley*, 2002]. Inverse isochron analysis of the NBUM10-45 data did not allow us to isolate the $^{40}Ar/^{36}Ar$ ratio of the trapped excess component, precluding determination of a precise date for the hornblende. We regard the ^{39}Ar abundance-weighted mean date for all steps in the release spectrum of 125.6 ± 6.1 Ma as our best (but imprecise) estimate for the apparent age of the hornblende. Because metamorphism of the Shyok Volcanic unit was restricted to lower greenschist facies, below the canonical $^{40}Ar/^{39}Ar$ hornblende closure temperature range of approximately 500–600°C [*Harrison*, 1981], we interpret this date as a minimum estimate of the igneous age of the Shyok Volcanic succession. Better constraints would require a more exhaustive search for datable zircons in a variety of units in the volcanic succession or the associated dikes.

5.2. Detrital U/Pb Zircon Constraints on the Provenance and Age of the Saltoro Molasse

We conducted a detrital zircon U/Pb laser ablation–inductively coupled plasma–mass spectrometry (LA-ICP-MS) study on sample BCUM12-105 collected from within the Saltoro Molasse in order to constrain its possible provenance and maximum age. This sample is from a sandy layer interpreted to be a channel, with both overlying and underlying conglomeratic strata. The 166 zircons dated from Saltoro Molasse sample BCUM12-105 range in $^{206}Pb/^{238}U$ age from Late Cretaceous to Neoarchean (Figure 8a). The majority of the grains from the sample ($n = 97$) define a single major mode with a mean $^{206}Pb/^{238}U$ age of 92.43 ± 0.24 Ma (Figure 8b). This is interpreted to be the oldest possible depositional age of the part of the Saltoro Molasse from which BCUM12-105 was collected. It seems unlikely that the actual depositional age is much younger because presumably postcollisional magmatic activity was ongoing in both the Kohistan-Ladakh and Karakoram blocks by at least 80 Ma [*Bosch et al.*, 2011; *Bouilhol et al.*, 2013; *Fraser et al.*, 2001; *Heuberger et al.*, 2007; *Jagoutz et al.*, 2009; *Jain and Singh*, 2008; *Ravikant et al.*, 2009; *Sen and Collins*, 2013; *Weinberg et al.*, 2000]. Unfortunately, the internal stratigraphy of the molasse is not well constrained; however, our sense is that this sample comes from the lower part of the succession. It is plausible, although we think unlikely, that the depositional age of the basal Saltoro Molasse could be older than approximately 92 Ma.

Compilations of zircon ages from the published literature for the Karakoram block and the Kohistan-Ladakh arc system in addition new data from this study are also shown in Figure 8a for comparison. We note that the majority of the studies of these potential source regions focused on granitic rocks, and any older country

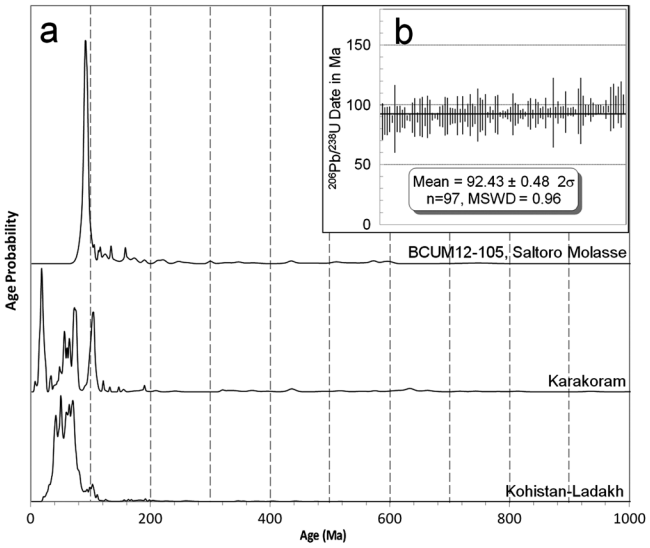

Figure 8. (a) Probability density plot for U/Pb zircon dates from the Karakoram and Kohistan-Ladakh blocks and the Saltoro Molasse. The plots are normalized such that the total area under curves is equal. Karakoram data ($n = 331$) are taken from bedrock and detrital samples from active drainages from *Fraser et al.* [2001], *Heuberger et al.* [2007], *Jain and Singh* [2008], *Lukens et al.* [2012], *Parrish and Tirrul* [1989], *Phillips et al.* [2004], *Ravikant et al.* [2009], *Weinberg et al.* [2000], and this study. Kohistan-Ladakh data ($n = 1342$) are from bedrock supplied by *Bosch et al.* [2011], *Bouilhol et al.* [2011, 2013], *Heuberger et al.* [2007], *Jagoutz et al.* [2009], *Khan et al.* [2009], *Ravikant et al.* [2009], and *Sen and Collins* [2013]. BCUM12-105 ($n = 166$) data are from a detrital bedrock sample from the Saltoro Molasse within the SSZ. (b) Mean U/Pb age for the youngest zircon population in BCUM12-105; black horizontal line is shown at the mean age for the population.

rocks or inheritance are therefore likely underrepresented, skewing the probability density plots for these potential source regions toward younger dates. While the majority of ages from the Kohistan-Ladakh block are younger than the major mode of sample BCUM12-105, this mode overlaps in time with a small but significant mode of bedrock zircon dates from the Kohistan-Ladakh block (Figure 8a). It matches less well with the known distribution of zircon ages for the Karakoram block. In fact, at the time of the deposition of the molasse, the approximately 105–90 Ma mode in the Kohistan-Ladakh spectra would have been the most significant mode for that block, as all other larger modes reported from Kohistan-Ladakh are younger than BCUM12-105. Furthermore, 20 of the grains that form the major mode in sample BCUM12-105 fall in a time span for which there are no zircons of that date reported from the Karakoram block, and there are only three reported zircon grains from the Karakoram block in the date range of 95–85 Ma. We tentatively conclude that the most likely source region for most of the detrital zircons in the youngest mode of the Saltoro Molasse is the Kohistan-Ladakh block but caution that the bedrock U/Pb zircon database for the Karakoram is sparse compared to those of other potential source regions and the full spectrum of potential Karakoram source region ages may not yet be known.

Both the Karakoram and Kohistan-Ladakh blocks seem viable contributors to the Early Cretaceous through Triassic zircon population present in the Saltoro Molasse. The Kohistan-Ladakh block population does contain a few Cambrian or older zircon grains that may have been the sources for some of the Cambrian or older crystals in the Saltoro Molasse, but a higher proportion of the Karakoram block zircons are Cambrian or Precambrian, making the Karakoram block the most likely source for these older grains. Given that zircons with a Th/U > 0.5 are most likely igneous [*Hoskin and Schaltegger*, 2003], the dates from BCU12-105 are interpreted to represent igneous activity throughout the entire range of dates represented in the molasse sample (Figure 9). Significant numbers of zircons with much lower Th/U also exist, which may indicate that both igneous and metamorphic zircons are included in the population. The similar correlations of Th/U scatter with $^{206}Pb/^{238}U$ date are also seen in the Early Paleozoic and Precambrian zircons we dated from Karakoram block samples (see below). Given that (1) the Saltoro Molasse is deposited on rocks likely originally deposited or erupted within or adjacent to the Ladakh arc, (2) the most abundant zircons in the studied Saltoro molasse sample appear to come from a Ladakh arc source, and (3) the Karakoram block provides a better match for observed Early Paleozoic and Precambrian zircons in the molasse sample, we interpret the Saltoro Molasse to be a postcollisional unit.

5.3. U/Pb LA-ICP-MS Zircon Bedrock Geochronology

5.3.1. Karakoram Block Paragneiss

Sample NBNU10-41, a sheared Karakoram block paragneiss collected within the Karakoram fault zone, contained euhedral zircons with both patchy and oscillatory zoning and—in most examples—direct evidence

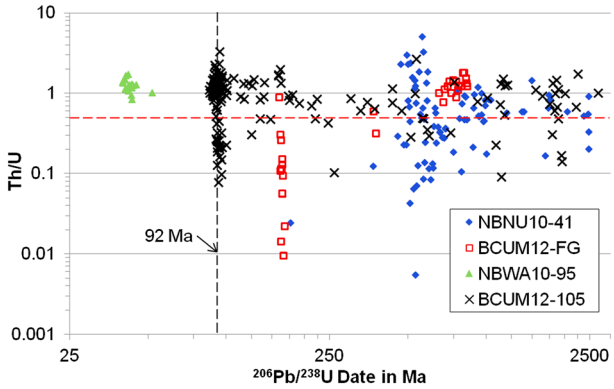

Figure 9. Th/U versus $^{206}Pb/^{238}U$ date plot for all zircon analyses from Saltoro Molasse sample BCUM12-105 and Karakoram block samples NBNU10-41, BCUM12-FG, and NBWA10-95. The horizontal red line is at Th/U = 0.5, above which zircons are most likely magmatic in origin [*Hoskin and Schaltegger*, 2003].

for overgrowths of rim material on inherited cores. A total of 44 zircon core analyses yielded $^{206}Pb/^{238}U$ dates ranging from approximately 500 to 2600 Ma (Figure 10a). The concordance or near concordance of many of these dates suggests the zircon cores are best interpreted as evidence of the incorporation of a range of Paleoproterozoic-Cambrian detrital zircons in the paragneiss protolith. Seventy-five rim analyses (Figure 10b) are scattered along or near concordia from approximately 1000 Ma to roughly 375 Ma. Many of these zircon rims have Th/U $\geq$ 0.5 and are likely igneous, but a significant number have much lower Th/U ratios and may be metamorphic (Figure 9). It is thus unclear from the data whether or not these zircon rims are all inherited detrital zircons or if some of the overgrowths could be related to early phases of metamorphism in the Karakoram block. One zircon rim in the large population we analyzed yielded an unusually young (177.0 ± 3.0 Ma) $^{206}Pb/^{238}U$ date and Th/U ratio of 0.02, which we tentatively interpret as indicating prograde metamorphism in the Karakoram block as recently as the Early Jurassic.

Thirty-three zircons from a granite sample ascribed to the Karakoram block (BUM12-FG; Figure 3) yielded a distribution of concordant and near-concordant dates similar to the rim population of Karakoram block sample NBNU10-41 (Figure 10c). The sample contained euhedral zircons with both patchy and oscillatory zoning and —in most examples—is direct evidence for overgrowths of rim material on inherited zircon cores. One significant difference is that the 14 youngest grains are concordant with one another, yielding an error-weighted mean $^{206}Pb/^{238}U$ date of 162.8 ± 1.2 Ma (2σ; Figure 10d). We interpret this mean date as the crystallization age of the granite and the older zircons as indicative of inheritance of older igneous and possibly metamorphic zircons (Figure 9). Unfortunately, sample BUM12-FG was not collected from an outcrop but instead from a rockslide below an inaccessible outcrop occurring in the hanging wall of the structure we map as the MKT, the Waris thrust (Figure 3). The similarity of rock types present in such rockfalls with unquestionable outcrops of the Karakoram block northeast of the Karakoram fault trace was the primary basis for our interpretation of the rocks above the Waris thrust in the Saltoro Range as belonging to the Karakoram block, but the similarity in inherited or detrital zircon age populations in NBNU10-41 and BUM12-FG lends credence to that interpretation.

5.3.2. Felsic Aplitic Dike Cutting the Shyok Volcanics-Saltoro Molasse Contact

One sample (BCUM12-146a, collected from sampling locality BCUM12-146 shown on Figure 3) was collected from an aplitic dike that cuts the unconformity between the Shyok Volcanics and Saltoro Molasse (Figure 11). Zircons from this sample are mostly euhedral and concentrically zoned. Three of these zircon grains were U/Pb LA-ICP-MS dated, one with a distinctive core and two with no obvious cores. A total of five core and rim $^{206}Pb/^{238}U$ analyses from the three zircons yielded statistically indistinguishable dates. In fact, the data for all zircons from this sample are concordant (Figure 10e), yielding a mean $^{206}Pb/^{238}U$ date of 85.2 ± 3.8 Ma (Figure 10f). We interpret this date as the igneous age of the dike from which BCUM12-146a was collected and also, due to the crosscutting relationship between the dike and the Shyok Volcanics-Saltoro Molasse unconformity, a minimum bound of the age of the Saltoro Molasse. Coupled with the approximately 92 Ma minimum age of detrital zircons in the molasse reported above, this date is consistent with Saltoro Molasse deposition beginning in the early Late Cretaceous.

5.3.3. Granites Intruding the SSZ

Two samples of granites cutting SSZ lithologies were collected for U/Pb geochronology: BCUM12-97, which intrudes the Shyok Volcanic unit, and BCUM12-135, which intrudes the Saltoro Formation (Figure 3). Both samples contained euhedral, concentrically zoned zircons, but only sample BCUM12-135 contained some crystals with obvious inherited cores. BCUM12-97 zircons are concordant (Figure 12a), and 24 $^{206}Pb/^{238}U$ dates for these zircon crystals have statistically indistinguishable results (Figure 12b) with a mean of 84.79 ± 0.68 Ma,

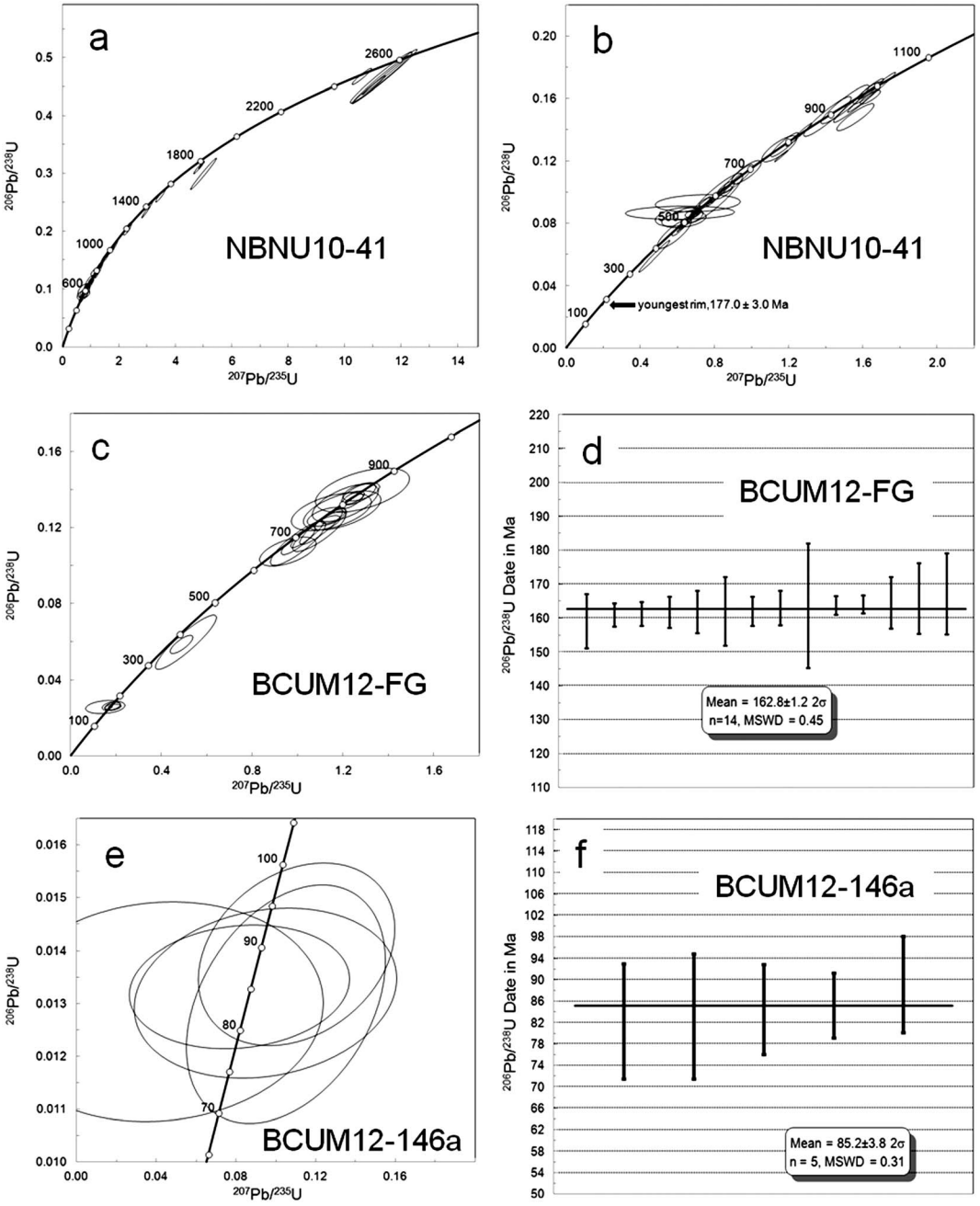

Figure 10. U/Pb zircon data from the SSZ. (a) Concordia diagram for cores from Karakoram affinity schist sample NBNU10-41. (b) Concordia diagram for rims from NBNU10-41. (c) Concordia diagram for all grains from Karakoram affinity granitic rockfall sample BCUM12-FG. (d) Mean age and dates for youngest population from BCUM12-FG. (e) Concordia diagram for all analyses from SSZ intruding dike sample BCUM12-146a. (f) Mean age and dates for all analyses from BCUM12-146a.

which is interpreted to be the intrusive age of this granite. Although sample BCUM12-135 zircon cores yield Mesoproterozoic dates (Figure 12c), the majority ($n = 23$) of the $^{206}Pb/^{238}U$ zircon dates in this rock are statistically indistinguishable with a mean of 86.05 ± 0.67 Ma (Figure 12d), which is the interpreted igneous age of this body. These granites, in addition to the 85.2 ± 3.8 Ma aplite dike sample (BCUM12-146a) also dated, suggest that Late Cretaceous (80–90 Ma) felsic igneous activity was widespread across all elements of the SSZ, providing a minimum age for amalgamation of the units within the suture zone. The Tirit Granite (Figure 3), for which *Upadhyay* [2008] reported a 71.40 ± 0.36 Ma (2σ) thermal ionization mass spectrometry U/Pb zircon age and *Weinberg et al*. [2000] reported a 68 ± 1 Ma (2σ) ion microprobe U-Pb zircon

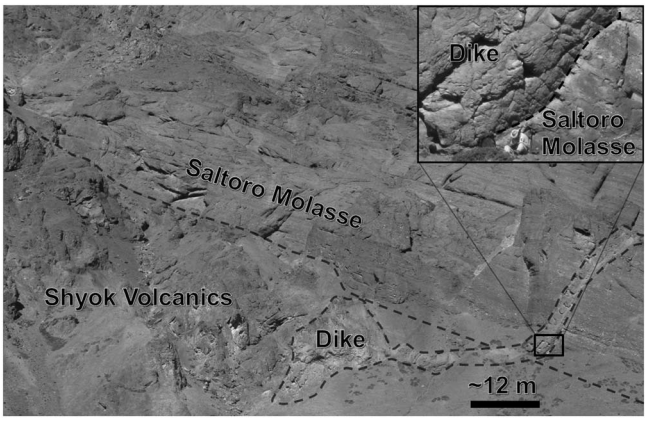

Figure 11. Field photo showing sampling site 146. The field of view looks west slopes away at an approximately 45° angle. The dike is approximately 4 m wide where it enters the Saltoro Molasse. Call-out shows the sampling location of BCUM12-146a with geologist for scale.

age, appears to be indicative of even more recent Cretaceous magmatism. There is no geochronologic evidence at present that plutons of equivalent age to the main Paleocene-Eocene intrusive phase of the Ladakh batholith occur in the SSZ.

5.3.4. Late Granodiorite Intruding the Karakoram Block

The youngest intrusive rock encountered in our study (NBWA10-95; Figure 3) is an undeformed granodiorite that intrudes older rocks of the Karakoram block and is cut by the Waris thrust. Eighteen euhedral zircons showing oscillatory zoning from this sample were dated. They yielded statistically indistinguishable $^{206}Pb/^{238}U$ results with a mean of 42.0 ± 1.7 Ma (Figure 12e), which we interpret as the rock's crystallization age; all zircons from this sample have Th/U > 0.5, indicating an igneous origin (Figure 9). The fact that this granodiorite is cut by the Waris thrust confirms that the thrust is one of the youngest structures in the study area, cut only by the Karakoram fault system.

6. Discussion and Conclusions

Prior to tectonic activity on the Shyok suture zone, the major nonoceanic crustal elements currently exposed to the southwest and northeast (Ladakh and Karakoram, respectively) were separated by part of the Neotethys Ocean basin. Although Late Cretaceous-Miocene igneous activity in the Ladakh Range apparently took place in a continental arc environment [*St-Onge et al*., 2010], several researchers interpret older igneous activity in Ladakh and the correlative Kohistan arc to the west as happening in an oceanic arc environment [e.g., *Burg*, 2011; *Bouilhol et al*., 2013]. We follow this argument in postulating that the Shyok suture zone manifests docking of this island arc with a Eurasian margin characterized by the Karakoram continental arc. Our U/Pb geochronologic data from Karakoram block elements in the Saltoro Range confirm that this arc was well established by Early-Middle Jurassic times.

Most rock packages in the SSZ of the Saltoro Range represent volcanic and sedimentary rocks deposited in a near-marine or marine environment (Shyok Volcanics and Saltoro Formation) or rocks interpreted as indicative of either a subduction complex or a tectonic unit related to suturing (the Mélange unit). As noted above, research in the along-strike equivalent of the SSZ in Pakistan led *Robertson and Collins* [2002] to propose that likely equivalents of our Shyok Volcanics and Saltoro Formation (their Pakora Formation) were deposited in a proximal back-arc basin environment of the Kohistan-Ladakh island arc, and we find such an interpretation equally suitable for the Saltoro Range exposures. Unfortunately, the eruptive age of the Shyok Volcanics is only constrained to $\geq 125.6 \pm 6.1$ (2σ) Ma by a $^{40}Ar/^{39}Ar$ date on an apparently igneous amphibole from a hypabyssal dike intrusive cutting that unit. We infer, however, that this dike intruded late in the eruptive history of the Shyok Volcanics, such that the volcanic unit is quite likely Early Cretaceous in age. Our data provide no direct constraints on the age of the overlying Saltoro Formation in the Saltoro Range, but fossils identified by *Upadhyay* [2014] suggest that deposition was ongoing over at least a portion of the Albian-Aptian interval.

At first glance, Cretaceous ages for the Shyok Volcanic unit and the Saltoro Formation might suggest a closer affinity of these units to the Karakoram block rather than the Kohistan-Ladakh block. However, both *Rolland et al*. [2000] and *Robertson and Collins* [2002] identified a similar succession immediately to the west that they correlated with the Kohistan-Ladakh block. These authors, as well as *Upadhyay* [2014] and *Weinberg et al*. [2000], explicitly interpreted the Shyok Volcanic unit and Saltoro Formation as having formed in association with the Kohistan-Ladakh block. This interpretation is supported by some additional geological evidence in our field area. The Shyok Volcanic unit and the Saltoro Formation are separated from the Ladakh block by

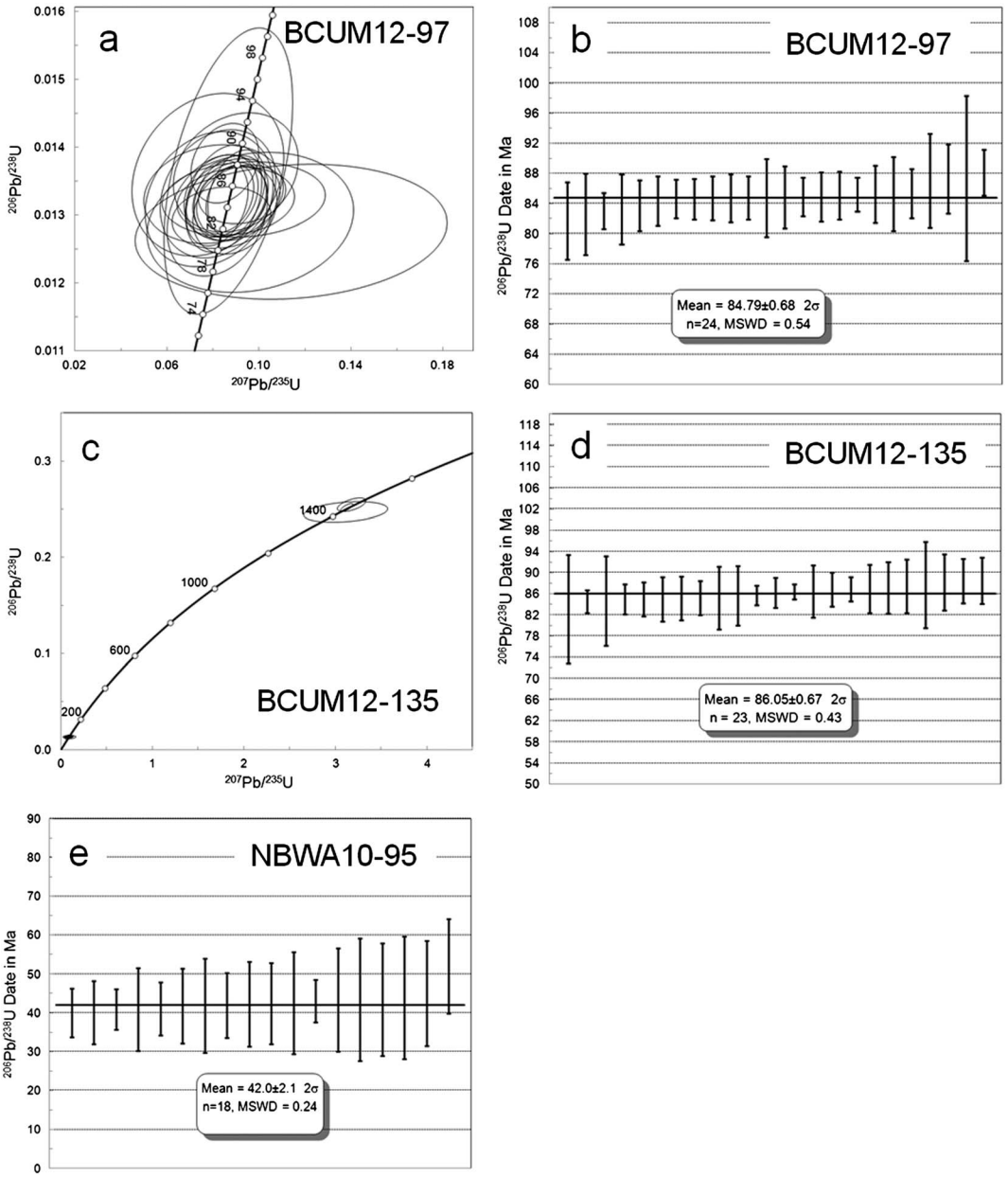

Figure 12. (a) Concordia diagram for all grains from SSZ intruding granitic sample BCUM12-97. (b) Mean age and dates for all grains from BCUM12-97. (c) Concordia diagram for all grains from SSZ intruding granitic sample BCUM12-135. (d) Mean age and dates for youngest population from BCUM12-135. (e) Mean age and dates for all grains from Karakoram affinity granitic sample NBWA10-95.

the steeply dipping Khalsar thrust. Barring significant rotation of that structure after its activity—something for which we have no evidence—it seems unlikely that the displacement on that structure was large enough to juxtapose units deposited near the Karakoram block against the Kohistan-Ladakh block. In light of the fact that we have no evidence from our study area to the contrary, we accept the interpretations of previous workers that the Shyok Volcanic unit and Saltoro Formation constitute some of the oldest preserved portion of the Kohistan-Ladakh block and are not part of the Karakoram block.

If our interpretation is correct that marine units of the Shyok Volcanics and Saltoro Formation are Cretaceous, the age of suturing of the Kohistan-Ladakh arc to Eurasia can be no older that Early Cretaceous. A minimum age constraint is provided by the Saltoro Molasse, which is interpreted as largely or completely deposited in a postsuturing continental environment. Unless existing zircon data sets for the Kohistan-Ladakh and

Karakoram arcs are not indicative of the complete range of zircon U/Pb dates from the two distinctive crustal blocks, the simplest interpretation of the detrital zircon suite in the studied sample of the Saltoro Molasse (BCUM12-105) is that the molasse has a mixed zircon provenance from both Kohistan-Ladakh and the Karakoram even though the age distribution for our sample does not perfectly match that of either potential source block. The youngest U/Pb detrital zircon subpopulation within sample BCUM12-105 implies deposition of most or all of the Saltoro Molasse at or after approximately 92 Ma, whereas the approximately 85 Ma $^{206}Pb/^{238}U$ date of a crosscutting dike (BCUM12-146a) provides a minimum age. Following this line of reasoning, the Shyok suturing event must be no younger than Late Cretaceous (Santonian-Turonian). While this model is consistent with all of our data and the presently available and published zircon U/Pb data sets for both the Karakoram and Kohistan-Ladakh blocks, it must be noted that the data sets for both blocks are still sparse, and future data sets will be needed to further evaluate the model. A Cretaceous age for the Shyok suture zone is consistent with conventional wisdom [e.g., *Clift et al*., 2002; *Petterson and Windley*, 1985; *Treloar et al*., 1989; *Searle*, 1991; *Searle et al*., 1997; *Robertson and Collins*, 2002; *Burtman*, 2010; *Rehman et al*., 2011; *Thanh et al*., 2012], but it is inconsistent with two recent papers arguing for an approximately 50 or approximately 40 Ma age. *Khan et al*. [2009] inferred that the Kohistan-Ladakh intraoceanic arc collided with India at approximately 65–61 Ma and Kohistan-Ladakh-India collided at approximately 50 Ma with the southern margin of Eurasia along the Shyok suture. To support this interpretation, they inferred that paleomagnetic data from India placed the Kohistan-Ladakh arc and the northern Indian margin near the equator at approximately 65–61 Ma, far south of the southern margin of Eurasia. More recently, *Bouilhol et al*. [2013] employed U/Pb geochronology and the evolution of Hf, Nd, and Sr isotopic signatures with time in Kohistan-Ladakh plutonic rocks to argue instead for approximately 50 Ma collision of Kohistan-Ladakh with India, followed by approximately 40 Ma closure along the Shyok suture.

Neither the *Khan et al*. [2009] or *Bouilhol et al*. [2013] models can be reconciled with our data, which appear to imply that the continental Saltoro Molasse began to be deposited across the Shyok suture in the Late Cretaceous. Is there an alternative interpretation of our data that might eliminate this inconsistency? While the Saltoro Molasse was certainly not deposited in an oceanic setting and we infer from our detrital zircon U/Pb data that it contains sediment shed from both the Karakoram and Kohistan-Ladakh blocks, an argument could be made that existing U/Pb zircon data sets from these blocks are not yet sufficiently comprehensive to permit definitive provenance interpretations for this molasse. For example, a later collision between Kohistan-Ladakh and the Karakoram might be possible if the Saltoro Molasse was deposited on an emergent part of the Kohistan-Ladakh block, and that block contained an as-yet uncharacterized source for the Precambrian zircons in the molasse. Further evaluation of such possibilities will require more spatially comprehensive mapping of U/Pb age variations in the Karakoram and Ladakh blocks.

At the same time, there are good reasons for objective skepticism about models that invoke a Tertiary age for Shyok suturing. The *Khan et al*. [2009] model depends heavily on a paleolatitude estimate for the Kohistan arc derived from previously published paleomagnetic data for Paleocene volcanic rocks in northern Pakistan [*Ahmed et al*., 2000]. Unfortunately, those data were obtained from deformed and remagnetized rocks, calling into question the robustness of the estimated paleolatitude and the authors' rough estimate of the timing of the remagnetization event. Additionally, the *Khan et al*. [2009] model fails to take into account paleomagnetic evidence that is suggestive that Kohistan-Ladakh arc and Eurasia were close to each other in the Middle to Late Cretacous [*Rehman et al*., 2011; *Zaman and Torii*, 1999]. It is fair to say that the Cretaceous-early Cenozoic paleolatitudes of the Kohistan-Ladakh arc remain very poorly constrained at present. In our opinion, any robust paleomagnetic model for timing of the Shyok suture needs to incorporate data from the Karakoram block, for which there are scant data.

The *Bouilhol et al*. [2013] model interprets a distinctive change in Ladakh arc isotopic geochemistry at approximately 40 Ma—indicative of a greater component of crustal contamination—as unambiguously related to southward underthusting of the Karakoram block beneath the Kohistan-Ladakh block during Shyok suturing. Indeed, direct field evidence exists for some limited degree of southward underthrusting of suture zone lithologies in the Saltoro Range beneath the Ladakh block along the Khalsar thrust (Figure 3). However, if this—or a similarly oriented structure—carries Karakoram rocks deeply enough to contaminate the source regions of Ladakh plutons after 40 Ma, it could have easily done so long after Shyok suturing. An even simpler explanation for the change in isotopic signature might be that it marks the arrival of Indian continental lithosphere within or above the Ladakh magma source area, especially inasmuch as most published

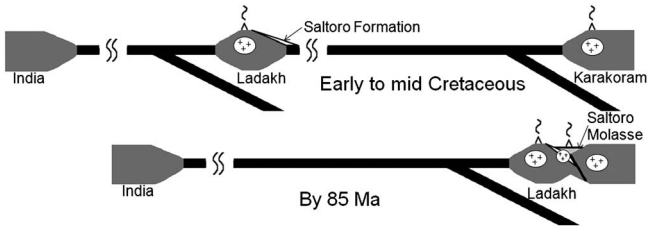

Figure 13. Tectonic cartoon showing our model for the timing of the formation of the SSZ.

models for the evolution of this part of the Himalaya feature collision of the Indian and Eurasian plates as well as ultrahigh pressure metamorphism of India's leading edge only 10 or so million years earlier [e.g., *Donaldson et al*., 2013; *Najman et al*., 2010; *St-Onge et al*., 2013]. Similar Cretaceous-middle Tertiary geochemical transitions have been documented for the Gangdese arc in southern Tibet, and those have been interpreted as indicative of Indian plate crustal contamination or partial melting [e.g., *Jiang et al*., 2014]. On balance, we regard the Cretaceous age for the Shyok suture indicated by our study as being more consistent with regional geological constraints than either of the Tertiary ages proposed by *Khan et al*. [2009] and *Bouilhol et al*. [2013]. If correct, our interpretation lends support to more traditional models of the Cretaceous-early Tertiary collisional history of this sector of the Himalaya, which hold that (1) the early Kohistan-Ladakh island arc was incorporated into the southern margin of Eurasia in the Cretaceous and afterward evolved as a continental arc over a north facing subduction zone and (2) final closure of the Neo-Tethys Ocean occurred along the Indus suture to the south (Figure 13).

Existing geochronologic data from NW India suggest that Cretaceous accretion of the Ladakh arc may have resulted in a temporary reduction in activity within the Karakoram arc, but a northward expansion of igneous activity beyond the Ladakh Range and into the Shyok suture zone, accounting for the Tirit Granite and other bodies described and dated as part of our study. Such expansion is consistent with a model in which the subduction angle beneath the Ladakh arc flattened and the subduction rate increased in order to accommodate an additional component of India-Eurasia convergence rate after cessation of subduction beneath the Karakoram.

Apparent confirmation of a Cretaceous age for the Shyok suture strongly suggests that this suture is correlative with the similarly aged Bangong suture of central Tibet [*Kapp et al*., 2007; *Liu et al*., 2014] but not the Cenozoic Yarlung suture [*Najman et al*., 2010]. This correlation supports traditionally accepted tectonic scenarios in which a continuous, "Transhimalayan," Andean-type arc system characterized the southern margin of Eurasia and accommodated northward subduction of the Neo-Tethys Ocean basin prior to India-Eurasia collision [e.g., *Hodges*, 2000]. Today the remnants of this system are preserved as Late Cretaceous-Paleocene, intrusive and extrusive igneous rocks of the Gangdese arc in southern Tibet and the Kohistan-Ladakh arc in NW India and Pakistan.

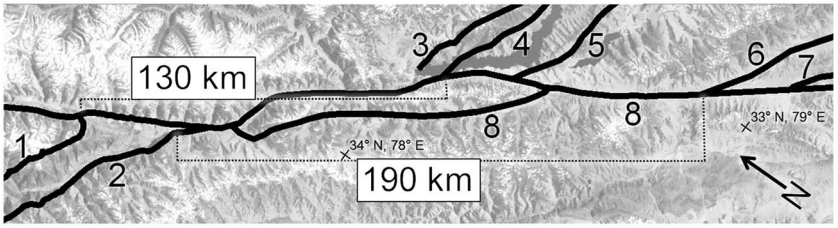

Figure 14. Our preferred offsets along the Karakoram fault correlating ophiolitic segments of the SSZ and Bangong suture zone superimposed over Google Earth imagery, with zones/boundaries of possible correlation labeled. The position of this figure is shown in Figure 1. (1) The Waris thrust (MKT) and northern ophiolitic mélange zone in the SSZ. (2) The Khalsar thrust and the southern ophiolitic mélange zone in the SSZ. (3) Northern extent of the Bangong suture zone as mapped by *Phillips* [2008] and *Van Buer et al*. [2015]. (4) Northern extent of ophiolitic mélange extended to the west from *Kapp et al*. [2003] and *Liu et al*. [2014] and also the southern extent of the Bangong suture zone from *Phillips* [2008] and *Van Buer et al*. [2015]. (5) Southern extent of ophiolitic mélange extended to the west from *Kapp et al*. [2003] and *Liu et al*. [2014]. (6) Northern extent of ophiolitic mélange in the Shequanhe suture zone from *Kapp et al*. [2003]. (7) Southern extent of ophiolitic mélange in the Shequanhe suture zone from *Kapp et al*. [2003]. (8) Karakoram Fault. The offset of 130 km corresponds to the position of the Waris thrust and associated ophiolitic mélange within the SSZ and our proposed correlation to the northernmost mapped extent of ophiolitic mélange within the Bangong suture zone. The offset of 190 km corresponds to the position of the Khalsar and associated ophiolitic mélange within the SSZ and our proposed correlation to the northernmost mapped extent of ophiolitic mélange within the Shequanhe suture segment of the Bangong suture zone.

Correlation of the Shyok and Bangong sutures across the Karakoram Fault constrains the total slip on that structure. We note that the SSZ immediately southeast of our study area includes two distinctive belts of ophiolitic material, truncated by the Karakoram Fault, which have similar appearance to two belts of what has been mapped by others [*Kapp et al*., 2003; *Liu et al*., 2014] as "ophiolitic mélange" in the Bangong suture, where the southern of the two ophiolite bearing belts is sometimes referred to as the Shequanhe suture. These belts are also truncated by the Karakoram Fault in such a way as to suggest correlation with the belts in the Shyok suture zone (Figure 14). Matching the northernmost of these belts across the fault suggests an approximate total offset of approximately 130 km. The same exercise using the southernmost belts suggests an offset of approximately 190 km. The range in offsets likely results from contractional deformation, such as along the MKT, that postdates the initiation of the Karakoram Fault. These estimates can be compared with previous estimates of maximum Karakoram Fault offset ranging from approximately 120 km to approximately 200 km [*Searle*, 1996; *Searle et al*., 1998; *Lacassin et al*., 2004].

Acknowledgments
Additional details regarding analytical techniques and detailed data tables may be found in the supporting information file. We gratefully acknowledge that funding for the research reported here was provided by the U.S. National Science Foundation through awards EAR 1007929 (Tectonics) and EAR 0642731 (Sedimentary Geology and Paleobiology). We thank the Arizona LaserChron Center, supported by NSF-EAR 1338583, for the use of their facilities and C.P. Dorjay for the field and logistical support. Associate Editor Paul Kapp and two anonymous reviewers are thanked for providing useful feedback on the initial submission of this paper that substantially improved the final version.

References

Ahmed, M. N., M. Yoshida, and F. Yoshiki (2000), Paleomagnetic study of Utror volcanic formation; remagnetizations and postfolding rotations in Utror area, Kohistan arc, northern Pakistan, *Earth, Planets Space*, *52*, 425–36.

Aitchison, J. C., X. Xia, A. T. Baxter, and J. R. Ali (2011), Detrital zircon U-Pb ages along the Yarlung-Tsangpo suture zone, Tibet: Implications for oblique convergence and collision between India and Asia, *Gondwana Res.*, *20*, 691–709, doi:10.1016/j.gr.2011.04.002.

Allen, T., and C. P. Chamberlain (1991), Metamorphic evidence for an inverted crustal section, with constraints on the Main Karakoram Thrust, Baltistan, northern Pakistan, *J. Metamorph. Geol.*, *9*(4), 403–418, doi:10.1111/j.1525-1314.1991.tb00535.x.

Bosch, D., C. J. Garrido, O. Bruguier, B. Dhuime, J.-L. Bodinier, J. A. Padron-Navarta, and B. Galland (2011), Building an island-arc crustal section: Time constraints from a LA-ICP-MS zircon study, *Earth Planet. Sci. Lett.*, *309*, 268–279, doi:10.1016/j.epsl.2011.07.016.

Bouilhol, P., U. Schaltegger, M. Chiaradia, M. Ovtcharova, A. Stracke, J.-P. Burg, and H. Dawood (2011), Timing of juvenile arc crust formation and evolution in the Sapat Complex (Kohistan-Pakistan), *Chem. Geol.*, *280*, 243–256, doi:10.1016/j.chemgeo.2010.11.013.

Bouilhol, P., O. Jagoutz, J. M. Hanchar, and F. O. Dudas (2013), Dating the India-Eurasia collision through arc magmatic records, *Earth Planet. Sci. Lett.*, *366*, 163–175, doi:10.1016/j.epsl.2013.01.023.

Brown, E. T., R. Bendick, D. L. Bourles, V. Gaur, P. Molnar, G. M. Raisbeck, and F. Yiou (2002), Slip rates of the Karakorum Fault, Ladakh, India, determined using cosmic ray exposure dating of debris flows and moraines, *J. Geophys. Res.*, *107*(B9), 2192, doi:10.1029/2000JB000100.

Burg, J. P. (2011), The Asia–Kohistan–India collision: Review and discussion, in *Arc-Continent Collision*, edited by D. Brown and P. D. Ryan, pp. 279–309, Springer, Berlin.

Burtman, V. S. (2010), Tien Shan, Pamir, and Tibet: History and geodynamics of Phanerozoic oceanic basins, *Geotectonics*, *44*(5), 388–404.

Clift, P. D., R. Hannigan, J. Blusztajn, and A. E. Draut (2002), Geochemical evolution of the Dras-Kohistan Arc during collision with Eurasia: Evidence from the Ladakh Himalaya, India, *Island Arc*, *11*(4), 255–273.

Cooper, F. J., B. A. Adams, C. S. Edwards, and K. V. Hodges (2012), Large normal-sense displacement on the South Tibetan fault system in the eastern Himalaya, *Geology*, *40*(11), 971–974, doi:10.1130/G33318.1.

Crawford, M. B., and M. P. Searle (1992), Field relationships and geochemistry of pre-collisional (India-Asia) granitoid magmatism in the central Karakoram, northern Pakistan, *Tectonophysics*, *206*, 171–192, doi:10.1016/0040-1951(92)90375-G.

DeCelles, P. G., P. Kapp, G. E. Gehrels, and L. Ding (2014), Paleocene-Eocene foreland basin evolution in the Himalaya of southern Tibet and Nepal: Implications for the age of initial India-Asia collision, *Tectonics*, *33*(5), 824–849, doi:10.1002/2014TC003522.

Donaldson, D. G., A. A. G. Webb, C. A. Menold, A. R. C. Kylander-Clark, and B. R. Hacker (2013), Petrochronology of Himalayan ultrahigh-pressure eclogite, *Geology*, *41*(8), 835–838, doi:10.1130/G33699.1.

Dunlap, W. J., and R. Wysoczanski (2002), Thermal evidence for Early Cretaceous metamorphism in the Shyok suture zone and age of the Khardung volcanic rocks, Ladakh, India, *J. Asian Earth Sci.*, *20*(5), 481–490, doi:10.1016/S1367-9120(01)00042-6.

Ehiro, M., S. Kojima, T. Sato, T. Ahmad, and T. Ohtani (2007), Discovery of Jurassic ammonoids from the Shyok suture zone to the northeast of Chang La pass, Ladakh, northwest India and its tectonic significance, *Isl. Arc*, *16*, 124–132, doi:10.1111/j.1440-1738.2007.00562.x.

Fraser, J. E., M. P. Searle, R. R. Parrish, and S. R. Noble (2001), Chronology of deformation, metamorphism, and magmatism in the southern Karakoram Mountains, *Geol. Soc. Am. Bull.*, *113*, 1443–1455, doi:10.1130/0016-7606(2001)113<1443:CODMAM>2.0.CO;2.

Harrison, T. M. (1981), Diffusion of ^{40}Ar in hornblende, *Contrib. Mineral. Petrol.*, *78*, 324–331.

Hastie, A. R., A. C. Kerr, J. A. Pearce, and S. F. Mitchell (2007), Classification of altered volcanic island arc rocks using immobile trace elements: Development of the Th-Co discrimination diagram, *J. Petrol.*, *48*, 2341–2357, doi:10.1093/petrology/egm062.

Heuberger, S., U. Schaltegger, J.-P. Burg, I. M. Villa, M. Frank, H. Dawood, S. Hussain, and A. Zanchi (2007), Age and isotopic constraints on magmatism along the Karakoram-Kohistan suture zone, NW Pakistan: Evidence for subduction and continued convergence after India-Asia collision, *Swiss J. Geosci.*, *100*, 85–107, doi:10.1007/s00015-007-1203-7.

Hodges, K. V. (2000), Tectonics of the Himalaya and southern Tibet from two perspectives, *Geol. Soc. Am. Bull.*, *112*, 324–350, doi:10.1130/0016-7606(2000)112<0324:TOTHAS>2.3.CO;2.

Hollocher, K., P. Robinson, E. Walsh, and D. Roberts (2012), Geochemistry of amphibolite-facies volcanics and gabbros of the Storen nappe in extensions west and southwest of Trondheim, western gneiss region, Norway: A key to correlations and paleotectonic settings, *Am. J. Sci.*, *312*, 357–416, doi:10.2475/04.2012.01.

Horton, F., and M. L. Leech (2013), Age and origin of granites in the Karakoram shear zone and Greater Himalaya Sequence, NW India, *Lithosphere*, *5*, 300–320, doi:10.1130/L213.1.

Hoskin, P. W. O., and U. Schaltegger (2003), The composition of zircon and igneous and metamorphic petrogenesis, *Rev. Mineral. Geochem.*, *53*, 27–62, doi:10.2113/0530027.

Jagoutz, O., J.-P. Burg, S. Hussain, H. Dawood, T. Pettke, T. Iizuka, and S. Maruyama (2009), Construction of the granitoid crust of an island arc Part I: Geochronological and geochemical constraints from the plutonic Kohistan (NW Pakistan), *Contrib. Mineral. Petrol.*, *158*, 739–755, doi:10.1007/s00410-009-0408-3.

Jagoutz, O., L. Royden, A. F. Holt, and T. W. Becker (2015), Anomalously fast convergence of India and Eurasia caused by double subduction, *Nat. Geosci.*, *8*(6), doi:10.1038/ngeo2418.

Jain, A. K., and S. Singh (2008), Tectonics of the southern Asian plate margin along the Karakoram shear zone: Constraints from field observations and U-Pb SHRIMP ages, *Tectonophysics*, *451*, 186–205, doi:10.1016/j.tecto.2007.11.048.
Ji, W.-Q., F.-Y. Wu, S.-L. Chung, J.-X. Li, and C.-Z. Liu (2009), Zircon U-Pb geochronology and Hf isotopic constraints on petrogenesis of the Gangdese batholith, southern Tibet, *Chem. Geol.*, *262*(3–4), 229–245, doi:10.1016/j.chemgeo.2009.01.020.
Jiang, Z. Q., et al. (2014), Transition from oceanic to continental lithosphere subduction in southern Tibet: Evidence from the Late Cretaceous-Early Oligocene (~91-30 Ma) intrusive rocks in the Chanang-Zedong area, southern Gangdese, *Lithos*, *196*, 213–231.
Jolliffe, I. T. (2002), *Principal Component Analysis*, 2nd ed., 32 pp, Springer, New York.
Juyal, K. P. (2006), Foraminiferal biostratigraphy of the Early Cretaceous Hundiri Formation, lower Shyok are, eastern Karakoram, India, *Curr. Sci.*, *91*, 1096–1101.
Kapp, P., M. A. Murphy, A. Yin, T. M. Harrison, L. Ding, and J. H. Guo (2003), Mesozoic and Cenozoic tectonic evolution of the Shiquanhe area of western Tibet, *Tectonics*, *22*(4), 1029, doi:10.1029/2001TC001332.
Kapp, P., P. G. DeCelles, G. E. Gehrels, M. Heizier, and L. Ding (2007), Geological records of the Lhasa-Qiangtang and Indo-Asian collisions in the Nima area of central Tibet, *Geol. Soc. Am. Bull.*, *119*, 917–932, doi:10.1130/B26033.1.
Kelley, S. (2002), Excess argon in K-Ar and Ar-Ar geochronology, *Chem. Geol.*, *188*(1–2), 1–22, doi:10.1016/S0009-2541(02)00064-5.
Khan, S. D., D. J. Walker, S. A. Hall, K. C. Burke, M. T. Shah, and L. Stockli (2009), Did the Kohistan-Ladakh island arc collide first with India?, *Geol. Soc. Am. Bull.*, *121*, 366–384, doi:10.1130/B26348.1.
Lacassin, R., et al. (2004), Large-scale geometry, offset and kinematic evolution of the Karakorum Fault, Tibet, *Earth Planet. Sci. Lett.*, *219*(3–4), 255–269.
Lister, G. S., and A. W. Snoke (1984), S-C mylonites, *J. Struct. Geol.*, *6*, 617–638.
Liu, W.-L., B. Xia, Y. Zhong, J.-X. Cai, J.-F. Li, H.-F. Liu, Z.-R. Cai, and Z.-L. Sun (2014), Age and composition of the Rebang Co and Julu ophiolites, central Tibet: Implications for the evolution of the Bangong Meso-Tethys, *Int. Geol. Rev.*, *56*, 430–447, doi:10.1080/00206814.2013.873356.
Lukens, C. E., B. Carrapa, B. S. Singer, and G. Gehrels (2012), Miocene exhumation of the Pamir revealed by detrital geothermochronology of Tajik Rivers, *Tectonics*, *31*, TC2014, doi:10.1029/2011TC003040.
McDermid, I. R. C., J. C. Aitchison, A. M. Davis, T. M. Harrison, and M. Grove (2002), The Zedong terrane: A Late Jurassic intra-oceanic magmatic arc wihin the Yarlung-Tsangpo suture zone, southeastern Tibet, *Chem. Geol.*, *187*, 267–277.
Najman, Y., et al. (2010), Timing of India-Asia collision: Geological, biostratigraphic, and palaeomagnetic constraints, *J. Geophys. Res.*, *115*, B12416, doi:10.1029/2010JB007673.
Parrish, R. R., and R. Tirrul (1989), U-Pb age of the Baltoro granite, northwest Himalaya, and implications for monazite U-Pb systematics, *Geology*, *17*, 1076–1079, doi:10.1130/0091-7613(1989)017<1076:UPAOTB>2.3.CO;2.
Petterson, M. G., and B. F. Windley (1985), Rb-Sr dating of the Kohistan arc-batholith in the Trans-Himalaya of north Pakistan, and tectonic implications, *Earth Planet. Sci. Lett.*, *74*, 45–57.
Phillips, R. J. (2008), Geological map of the Karakoram fault zone, Eastern Karakoram, Ladakh, NW Himalaya, *J. Maps*, *4*(1), 21–37.
Phillips, R. J., and M. P. Searle (2007), Macrostructural and microstructural architecture of the Karakoram Fault: Relationship between magmatism and strike-slip faulting, *Tectonics*, *26*, TC3017, doi:10.1029/2006TC001946.
Phillips, R. J., R. R. Parrish, and M. P. Searle (2004), Age constraints on ductile deformation and long-term slip rates along the Karakoram fault zone, Ladakh, *Earth Planet. Sci. Lett.*, *226*, 305–319, doi:10.1016/j.epsl.2004.07.037.
Rai, H. (1982), Geological evidence against the Shyok palaeo-suture, Ladakh Himalaya, *Nature*, *297*, 142–144, doi:10.1038/297142A0.
Rao, D. R., and H. Rai (2009), Geochemical studies of granitoids from Shyok tectonic zone of Khardung-Panamik Section, Ladakh, India, *J. Geol. Soc. India*, *73*, 553–566.
Ravikant, V., F.-Y. Wu, and W.-Q. Ji (2009), Zircon U-Pb and Hf isotopic constraints on petrogenesis of the Cretaceous-Tertiary granites in eastern Karakoram and Ladakh, India, *Lithos*, *110*, 153–166, doi:10.1016/j.lithos.2008.12.013.
Raz, U., and K. Honegger (1989), Magmatic and tectonic evolution of the Ladakh block from field studies, *Tectonophysics*, *161*, 107–118, doi:10.1016/0040-1951(89)90306-5.
Rehman, H. U., T. Seno, H. Yamamoto, and T. Khan (2011), Timing of collision of the Kohistan-Ladakh Arc with India and Asia: Debate, *Island Arc*, *20*, 308–328, doi:10.1111/j.1440-1738.2011.00774.x.
Rex, A. J., M. P. Searle, R. Tirrul, M. B. Crawford, D. J. Prior, D. C. Rex, and A. Barnicoat (1988), The geochemical and tectonic evolution of the central Karakoram, North Pakistan, *Philos. Trans. R. Soc. London*, *326*, 229–255.
Robertson, A. H. F., and A. S. Collins (2002), Shyok suture zone, N Pakistan: Late Mesozoic-Tertiary evolution of a critical suture separating the oceanic Ladakh Arc from the Asian continental margin, *J. Asian Earth Sci.*, *20*, 309–351, doi:10.1016/S1367-9120(01)00041-4.
Rolland, Y., A. Pecher, and C. Picard (2000), Middle Cretaceous back-arc formation and arc evolution along the Asian margin: The Shyok suture zone in northern Ladakh (NW Himalaya), *Tectonophysics*, *325*, 145–173, doi:10.1016/S0040-1951(00)00135-9.
Rolland, Y., G. Maheo, A. Pecher, and I. M. Vila (2009), Syn-kinematic emplacement of the Pangong metamorphic and magmatic complex along the Karakorum Fault (N Ladakh), *J. Asian Earth Sci.*, *34*(1), 10–25.
Rowley, D. B. (1996), Age of initiation of collision between India and Asia: A review of stratigraphic data, *Earth Planet. Sci. Lett.*, *145*(1–4), 1–13, doi:10.1016/S0012-821X(96)00201-4.
Schwab, M., et al. (2004), Assembly of the Pamirs: Age and origin of magmatic belts from the southern Tien Shan to the southern Pamirs and their relation to Tibet, *Tectonics*, *23*, TC4002, doi:10.1029/2003TC001583.
Searle, M. P. (1991), *Geology and Tectonics of the Karakoram Mountains*, John Wiley, Chichester, U. K.
Searle, M. P. (1996), Geological evidence against large-scale pre-Holocene offsets along the Karakoram Fault: Implications for the limited extrusion of the Tibetan Plateau, *Tectonics*, *15*, 171–186, doi:10.1029/95TC01693.
Searle, M. P., and R. Tirrul (1991), Structural and thermal evolution of the Karakoram crust, *J. Geol. Soc.*, *148*, 65–82, doi:10.1144/gsjgs.148.1.0065.
Searle, M. P., R. I. Corfield, B. Stephenson, and J. McCarron (1997), Structure of the North Indian continental margin in the Ladakh-Zanskar Himalayas: Implications for the timing of obduction of the Spontang ophiolite, India-Asia collision and deformational events in the Himalaya, *Geol. Mag.*, *134*, 297–316.
Searle, M. P., R. F. Weinberg, and W. J. Dunlap (1998), Transpressional tectonics along the Karakoram fault zone, northern Ladakh: Constraints on Tibetan extrusion, in *Continental Transpressional and Transtensional Tectonics*, *Geol. Soc. London, Spec. Publ.*, vol. 135, edited by R. E. Holdsworth, R. A. Strachan, and J. F. Dewey, pp. 307–326, Geol. Soc. London, London.
Searle, M. P., M. A. Khan, J. E. Fraser, S. J. Gough, and M. Q. Jan (1999), The tectonic evolution of the Kohistan-Karakoram collision belt along the Karakoram Highway transect, north Pakistan, *Tectonics*, *18*, 929–949, doi:10.1029/1999TC900042.
Searle, M. P., R. R. Parrish, A. V. Thow, S. R. Noble, R. J. Phillips, and D. J. Waters (2010), Anatomy, age and evolution of a collisional mountain belt: The Baltoro granite batholith and Karakoram Metamorphic Complex, Pakistani Karakoram, *J. Geol. Soc.*, *167*, 183–202, doi:10.1144/0016-76492009-043.

Sen, K., and A. S. Collins (2013), Dextral transpression and late Eocene magmatism in the trans-Himalayan Ladakh Batholith (North India): Implications for tectono-magmatic evolution of the Indo-Eurasian collisional arc, *Int. J. Earth Sci.*, *102*, 1895–1909, doi:10.1007/s00531-012-0826-8.

St-Onge, M. R., N. Rayner, and M. P. Searle (2010), Zircon age determinations for the Ladakh batholith at Chumathang (Northwest India): Implications for the age of the India-Asia collision in the Ladakh Himalaya, *Tectonophysics*, *495*(3–4), 171–183.

St-Onge, M. R., N. Rayner, R. M. Palin, M. P. Searle, and D. J. Waters (2013), Integrated pressure-temperature-time constraints for the Tso Morari dome (Northwest India): Implications for the burial and exhumation path of UHP units in the western Himalaya, *J. Metamorph. Geol.*, *31*(5), 469–504.

Thanh, N. X., T. Itaya, T. Ahmad, S. Kojima, T. Ohtani, and M. Ehiro (2010), Mineral chemistry and K-Ar ages of plutons across the Karakoram Fault in the Shyok-Nubra confluence of northern Ladakh Himalaya, India, *Gondwana Res.*, *17*(1), 180–188, doi:10.1016/j.gr.2009.08.002.

Thanh, N. X., V. J. Rajesh, T. Itaya, B. Windley, S. Kwon, and C.-S. Park (2012), A Cretaceous forearc ophiolite in the Shyok suture zone, Ladakh, NW India: Implications for the tectonic evolution of the Northwest Himalaya, *Lithos*, *155*, 81–93, doi:10.1016/j.lithos.2012.08.016.

Treloar, P. J., D. C. Rex, P. G. Guise, M. P. Coward, M. P. Searle, B. F. Windley, M. G. Petterson, M. Q. Jan, and I. W. Luff (1989), K-Ar and Ar-Ar geochronology of the Himalayan collision in NW Pakistan: Constraints on the timing of suturing, deformation, metamorphism and uplift, *Tectonics*, *8*, 881–909, doi:10.1029/TC008i004P00881.

Tripathy-Lang, A., K. V. Hodges, M. C. van Soest, and T. Ahmad (2013), Evidence of pre-Oligocene emergence of the Indian passive margin and the timing of collision initiation between India and Eurasia, *Lithosphere*, *5*, 501–506, doi:10.1130/L273.1.

Upadhyay, R. (2008), Implications of U-Pb zircon age of the Tirit granitoids on the closure of the Shyok suture zone, northern Ladakh, India, *Curr. Sci.*, *94*, 1635–1640.

Upadhyay, R. (2014), Palaeogeographic significance of "Yasin-type" rudist and orbitolinid fauna of the Shyok Suture Zone, Saltoro Hills, northern Ladakh, India, *Curr. Sci.*, *106*, 223–228.

Valli, F., et al. (2008), New U-Th/Pb constraints on timing of shearing and long-term slip-rate on the Karakorum Fault, *Tectonics*, *27*, TC5007, doi:10.1029/2007TC002184.

Van Buer, N. J., O. Jagoutz, R. Upadhyay, and M. Guillong (2015), Mid-crustal detachment beneath western Tibet exhumed where conjugate Karakoram and Longmu–Gozha Co Faults intersect, *Earth Planet. Sci. Lett.*, *413*, 144–157.

van Hinsbergen, D. J. J., P. C. Lippert, G. Dupont-Nivet, N. McQuarrie, P. V. Doubrovine, W. Spakman, and T. H. Torsvik (2012), Greater India Basin hypothesis and a two-stage Cenozoic collision between India and Asia, *Proc. Natl. Acad. Sci. U.S.A.*, *109*(20), 7659–7664, doi:10.1073/pnas.1117262109.

Weinberg, R. F., and W. J. Dunlap (2000), Growth and deformation of the Ladakh batholith, northwest Himalayas: Implications for timing of continental collision and origin of calc-alkaline batholiths, *J. Geol.*, *108*, 303–320, doi:10.1086/314405.

Weinberg, R. F., W. J. Dunlap, and M. Whitehouse (2000), New field, structural and geochronological data from the Shyok and Nubra Valleys, northern Ladakh: Linking Kohistan to Tibet, *Geol. Soc. London, Spec. Publ.*, *170*, 253–275, doi:10.1144/GSL.SP.2000.170.01.14.

White, L. T., T. Ahmad, T. R. Ireland, G. S. Lister, and M. A. Forster (2011), Deconvolving episodic age spectra from zircons of the Ladakh Batholith, northwest Indian Himalaya, *Chem. Geol.*, *289*(3–4), 179–196.

Winchester, J. A., and P. A. Floyd (1977), Geochemical discrimination of different magma series and their differentiation products using immobile elements, *Chem. Geol.*, *20*(4), 325–343, doi:10.1016/0009-2541(77)90057-2.

Wu, F. Y., W. Q. Ji, J. G. Wang, C. Z. Liu, S. L. Chung, and P. D. Clift (2014), Zircon U-Pb and Hf isotopic constraints on the onset time of India-Asia collision, *Am. J. Sci.*, *314*, 548–579, doi:10.2475/02.2014.04.

Yin, A. (2010), Cenozoic tectonic evolution of Asia: A preliminary synthesis, *Tectonophysics*, *488*(1–4), 293–325, doi:10.1016/j.tecto.2009.06.002.

Yin, A., and T. M. Harrison (2000), Geologic evolution of the Himalayan-Tibetan orogen, *Annu. Rev. Earth Planet. Sci.*, *28*, 211–280, doi:10.1146/annurev.earth.28.1.211.

Zaman, H., and M. Torii (1999), Paleomagnetic study of Cretaceous red beds from the eastern Hindukush ranges, northern Pakistan; paleoarc construction of the Kohistan-Karakoram composite unit before the India-Asia collision, *Geophys. J. Int.*, *136*, 719–38.

Zhang, L.-L., C.-Z. Liu, F.-Y. Wu, W.-Q. Ji, and J.-G. Wang (2014), Zedong block revisited: An intra-oceanic arc within Neo-Tethys or a part of the Asian active continental margin?, *J. Asian Earth Sci.*, *80*, 34–55, doi:10.1016/j.jseaes.2013.10.029.